NAVAL POSTGRADUATE SCHOOL

MONTEREY, CALIFORNIA

THESIS

DETERMINATION OF EFFECTIVE AVAILABLE PRESSURE OF A ROTATING DETONATION ENGINE

by

Joshua A. Ten Eyck

June 2019

Thesis Advisor: Christopher M. Brophy
Co-Advisor: Joshua R. Codoni

Approved for public release. Distribution is unlimited.

THIS PAGE INTENTIONALLY LEFT BLANK

1. AGENCY USE ONLY *(Leave blank)*	**2. REPORT DATE** June 2019	**3. REPORT TYPE AND DATES COVERED** Master's thesis	
4. TITLE AND SUBTITLE DETERMINATION OF EFFECTIVE AVAILABLE PRESSURE OF A ROTATING DETONATION ENGINE		**5. FUNDING NUMBERS** N0001419WX01159	
6. AUTHOR(S) Joshua A. Ten Eyck			
7. PERFORMING ORGANIZATION NAME(S) AND ADDRESS(ES) Naval Postgraduate School Monterey, CA 93943-5000		**8. PERFORMING ORGANIZATION REPORT NUMBER**	
9. SPONSORING / MONITORING AGENCY NAME(S) AND ADDRESS(ES) Office of Naval Research , Arlington, VA 22203		**10. SPONSORING / MONITORING AGENCY REPORT NUMBER**	
11. SUPPLEMENTARY NOTES The views expressed in this thesis are those of the author and do not reflect the official policy or position of the Department of Defense or the U.S. Government.			
12a. DISTRIBUTION / AVAILABILITY STATEMENT Approved for public release. Distribution is unlimited.		**12b. DISTRIBUTION CODE** A	

13. ABSTRACT (maximum 200 words)

Rotating detonation engines (RDEs) offer improved efficiency over conventional ramjet engines due to their decreased combustion chamber size and increased pressure gain across the combustor; however, due to highly transient temperature and pressure conditions generated by the detonation wave, conventional total pressure diagnostics cannot resolve or survive the combustor flow field. A theoretical method of producing an effective available pressure (EAP), or time averaged total pressure capable of producing work, in an RDE was introduced by Kaemming and Paxson but was not experimentally tested. The objective of this thesis was to experimentally measure the EAP for an RDE for various exit area and inlet area conditions. A bluff body nozzle was designed and implemented to determine the base pressure drag created by the engine. This force was used in conjunction with the overall thrust to calculate the momentum thrust of the combustor. Utilizing steady state equations, the effective total chamber pressure was then calculated and compared to prior computational results. Results appear to capture the trends observed in the modeling but show deficits due to non-ideal mixing, incomplete combustion, and heat transfer. By closing this loop, a normalized metric to compare RDE efficiencies experimentally was implemented.

14. SUBJECT TERMS RDE, rotating detonation engine			**15. NUMBER OF PAGES** 121
			16. PRICE CODE
17. SECURITY CLASSIFICATION OF REPORT Unclassified	**18. SECURITY CLASSIFICATION OF THIS PAGE** Unclassified	**19. SECURITY CLASSIFICATION OF ABSTRACT** Unclassified	**20. LIMITATION OF ABSTRACT** UU

THIS PAGE INTENTIONALLY LEFT BLANK

DETERMINATION OF EFFECTIVE AVAILABLE PRESSURE OF A ROTATING DETONATION ENGINE

Joshua A. Ten Eyck
Ensign, United States Navy
BS, U.S. Naval Academy, 2018

Submitted in partial fulfillment of the
requirements for the degree of

MASTER OF SCIENCE IN ASTRONAUTICAL ENGINEERING

from the

**NAVAL POSTGRADUATE SCHOOL
June 2019**

Approved by: Christopher M. Brophy
      Advisor

      Joshua R. Codoni
      Co-Advisor

      Garth V. Hobson
      Chair, Department of Mechanical and Aerospace Engineering

iii

THIS PAGE INTENTIONALLY LEFT BLANK

ABSTRACT

Rotating detonation engines (RDEs) offer improved efficiency over conventional ramjet engines due to their decreased combustion chamber size and increased pressure gain across the combustor; however, due to highly transient temperature and pressure conditions generated by the detonation wave, conventional total pressure diagnostics cannot resolve or survive the combustor flow field. A theoretical method of producing an effective available pressure (EAP), or time averaged total pressure capable of producing work, in an RDE was introduced by Kaemming and Paxson but was not experimentally tested. The objective of this thesis was to experimentally measure the EAP for an RDE for various exit area and inlet area conditions. A bluff body nozzle was designed and implemented to determine the base pressure drag created by the engine. This force was used in conjunction with the overall thrust to calculate the momentum thrust of the combustor. Utilizing steady state equations, the effective total chamber pressure was then calculated and compared to prior computational results. Results appear to capture the trends observed in the modeling but show deficits due to non-ideal mixing, incomplete combustion, and heat transfer. By closing this loop, a normalized metric to compare RDE efficiencies experimentally was implemented.

THIS PAGE INTENTIONALLY LEFT BLANK

TABLE OF CONTENTS

LIST OF FIGURES

LIST OF TABLES

THIS PAGE INTENTIONALLY LEFT BLANK

LIST OF ACRONYMS AND ABBREVIATIONS

CEA	Chemical Equilibrium with Applications
CTAP	Capillary Tube Average Pressure
DAQ	Data Acquisition
EAP	Effective Available Pressure
NASA	National Aeronautics and Space Administration
NPS	Naval Postgraduate School
PGC	Pressure Gain Combustor
RDE	Rotating Detonation Engine
RPCL	Rocket Propulsion Combustion Laboratory
TC2	Test Cell 2

THIS PAGE INTENTIONALLY LEFT BLANK

ACKNOWLEDGMENTS

I would like to thank Dr. Chris Brophy, Dr. Josh Codoni, and LT Spencer Ewing for their countless hours of help and work to produce this thesis. I would also like to thank everyone who works at the Naval Postgraduate School Rocket Propulsion Combustion Laboratory for their time and patience while testing. Finally, I would like to thank my parents, Roseanne and Greg Ten Eyck, for pushing me to strive to be the best I can be.

THIS PAGE INTENTIONALLY LEFT BLANK

I.   INTRODUCTION

A.   OVERVIEW

Gas turbine engines have been utilized for decades by U.S. naval vessels and aircraft due to the relatively high power to weight ratio and simple maintenance [1]. However, this style of engine has begun to approach its maximum theoretical efficiency. In order to remain a military superpower, the United States must continue to push the envelope of technology. Though engines utilizing the Brayton Cycle, such as gas turbines, have proved effective, new thermodynamic cycles must be investigated to achieve noticeable improvement. The detonation cycle, a method of Pressure Gain Combustion (PGC), theoretically requires smaller engines to produce the same or larger thrust values. The result of implementing an improved thermodynamic cycle should directly map to longer range missiles and more fuel-efficient engines that will expand the United States' capabilities in an ever-changing military domain and may even potentially be implemented in rocket design to help propel mankind to new space horizons.

In a typical Brayton Cycle, air is compressed to a high pressure where fuel is injected and combusted, heating up the gas at nearly constant pressure. Then, the gas expands as it travels through a turbine or nozzle, delivering work or thrust out of the system. During combustion in the Brayton cycle, the temperature of the gaseous mixture increases as the pressure remains nearly constant. This isobaric heat addition limits the maximum possible work out of the system. Pressure Gain Combustion devices theoretically enables both a total pressure and temperature increase during the combustion process, therefore utilizing the detonation cycle, an engine is able to achieve more work out of the system [2].

Figure 1 depicts the P-v diagram of a typical Brayton Cycle overlaid with that of a detonation cycle [3]. The area bounded by the cycle process demonstrates the total work available of the system. The detonation cycle is able to utilize the increase in pressure to substantially increase the available work out of the system. The main difference between the Brayton cycle and detonation cycle is how the gas is combusted. Brayton Cycle engines utilize deflagration, subsonic combustion, which results in a nearly constant pressure heat

addition. Detonation combustion occurs when a propagating shockwave is coupled with a combustion front in which a portion of the heat released during the combustion process propels the shockwave. Because the shockwave results in an extremely sudden pressure rise, the pressure increase of the working fluid increases over nearly constant volume conditions [4]. The Brayton cycle also utilizes large compressors in order to condense the volume of the working fluid, whereas detonations inherently occur at nearly a constant volume. If implemented in a gas turbine system, the compression ratio of the compressor can be reduced since the detonation cycle does not require as much work to power the system [1]. The initial compression of the working fluid could also be achieved through a supersonic intake. The result is that a detonation cycle is theoretically able to achieve approximately a 30% more efficient engine than the Brayton Cycle [1].
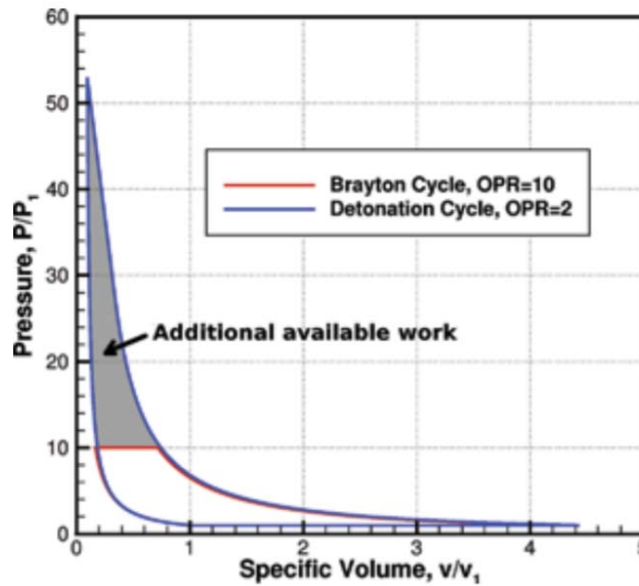
Figure 1.   P-v Diagram Comparing Brayton Cycle to Detonation
Cycle. Source: [1].

There are two devices being explored by researchers that utilize the detonation cycle, pulse detonation engines (PDEs) and rotating detonation engines (RDEs). In a PDE, the combustor is first filled with a reactive mixture, then a deflagration wave is ignited at the beginning of a long combustor tube. As the flow traverses down the pipe, wall obstacles

2

can be used to induce turbulence. The turbulence increases the flames burn area which in turn increases the flame speed and overall energy release rate. At a specific point, the deflagration wave may eventually transition to a detonation wave via the Deflagration-to-Detonation Transition (DDT) process [3]. Although, both PDEs and RDEs require a detonation wave to combust the fuel, PDEs also require the chamber to be purged between each combustion cycle, thus limiting the frequency at which the engine can operate and the capabilities of a PDE.

RDEs are different because the overall flow rates are constant. The fuel and air are mixed at the entrance to or slightly before the annular combustion chamber. As the detonation wave propagates, depicted in Figure 2, the fuel-oxidizer mixture is continuously injected, therefore only an initial detonation is necessary to produce a continuous wave. The wave is able to propagate around the combustor at high frequencies of greater than 3,000 Hz and depending on the reactivity of the mixture and fill height, can support multiple detonation waves [5].
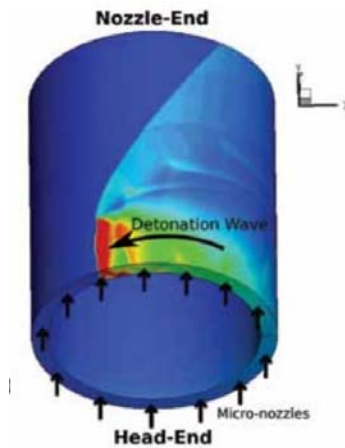
Figure 2.   Depiction of Detonation Channel in an RDE. Source: [1].

B.   MOTIVATION

Detonation engines are theoretically able to achieve much higher thermal efficiencies than typical air-breathing engines, however, comparing the two types of

devices is challenging. Conventional air-breathing engines, for a given mass flow rate, have steady state temperatures and pressures within the combustion chamber; whereas, RDEs have a detonation wave that travels circumferentially around the annular chamber at over 1 km/s. As the detonation wave propagates, the local temperature variation inside the chamber can be an order of magnitude higher than inlet and the pressure changes magnitude by up to 300 percent [6]. Due to the large variations in temperature and pressure, conventional methods of measuring chamber pressure for a typical combustion engine will not work on an RDE. Instead, a pressure term representative of the gross thrust created by the combustor under the quasi-steady state, homogeneous conditions—effective available pressure (EAP)—enables both experimental and computational analysis of an RDE to be directly compared to the stagnation chamber pressure analog of a typical combustion engine.

C.   OBJECTIVES

Literature reviews have shown that the ability to experimentally measure the effective pressure gain of an RDE has not yet been demonstrated. This work will be the first to calculate this value experimentally utilizing EAP calculations of an RDE located in Test Cell 2 of the Naval Postgraduate School's Rocket Propulsion Combustion Laboratory. The objectives of this thesis are listed as follow:

- Instrument the exit plane of an RDE with a bluff body exhaust nozzle to experimentally determine base drag.

- Instrument the detonation zone and chamber exit with ports to measure the time averaged static pressure.

- Determine the experimental EAP using combustor dimensions, gross thrust, and base drag values.

- Evaluate operability and pressure gain characteristics over three nozzle exit area ratios and three different air entrance gaps.

II. BACKGROUND

A. DETONATION ENGINES

Understanding the basics of detonation waves and RDEs is paramount for the measurement of EAP for an RDE. This section describes the structure and propagation of a detonation wave and how the energy is harnessed in an RDE to produce power in the form of thrust.

As stated in Lee's book *The Detonation Phenomenon*, a detonation wave is the coupling of a combustion wave and a shockwave [3]. The initial shockwave increases the temperature and pressure through adiabatic compression. Most of the reactants are dissociated by the leading shockwave in a region known as the induction zone. Directly after the induction zone, recombination of the reactants occurs and a combustion front forms. Figure 3 displays a 1-D detonation wave propagating through a flow.
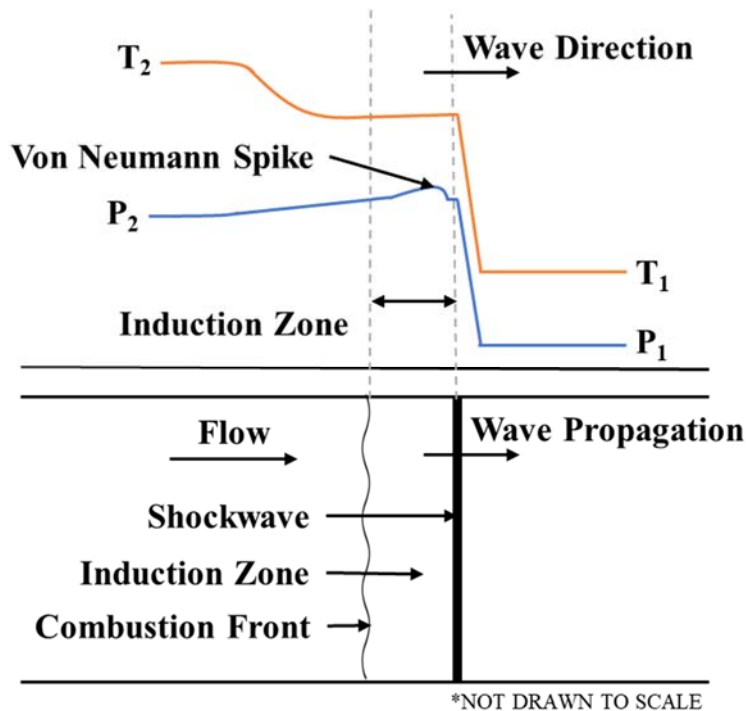
Figure 3.   Detonation Jump Conditions in a 1-D Flow. Adapted from [3].

As stated above, the wave is composed of three regions. First, an initial shock front compresses the fluid and causes a jump in both temperature and pressure. The speed of the flow in the induction zone is subsonic therefore, as the reactants combust in the combustion front, acoustic waves are sent through the induction zone, reinforcing the shockwave, thus increasing the pressure in the region; this phenomenon is known as the von Neumann Spike. Due to the sudden increase in pressure and temperature, the reactants start to react, initiating a chain reaction in the flow. As the fuel combusts, the temperature increases while the pressure remains relatively constant. The increased temperature and pressure across the detonation wave is known as the jump condition and can be idealized by a 1-D model is known as the Zeldovich-Neumann-Döring (ZND) model. Although this model is sufficient to capture the thermodynamic jump conditions, the nature and structure of a 3-D detonation wave is highly unstable and requires additional clarification.

The propagation of the shockwave and combustion front result in transverse waves that intersect with and locally increases the strength of the leading shock front. The intersections of the transverse waves, shock fronts, and a third equalizing shockwave known as the Mach stem, creates a triple point as depicted in Figure 4. At triple points, very high temperatures and pressures produce the environment for a strong combustion front to form [7]. Therefore, neither the leading shock front, nor the deflagrating combustion front are perfect isotropic waves; the constantly changing locations of triple points and traversing waves affect the fronts. The diamond shaped regions depicted in Figure 4 are known as detonation cells. The cell size, denoted as λ, is defined by the maximum width of a cell. Cell size is affected by the type of fuel as well as the mixture ratio of fuel to oxidizer.
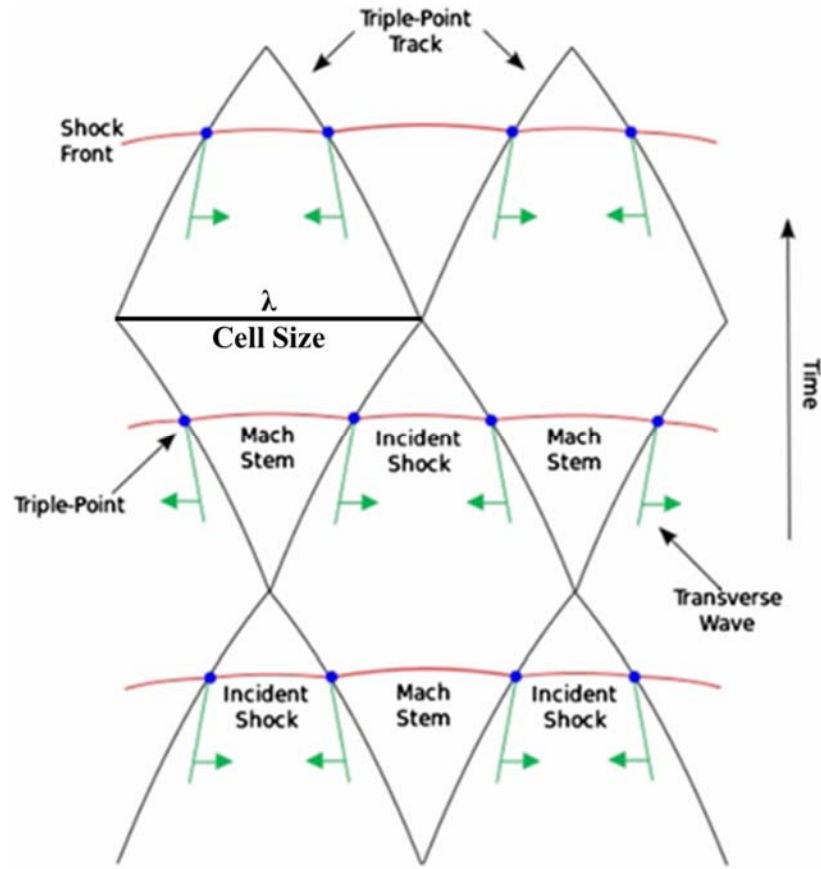
Figure 4.   Cell Structure of a Detonation Shockwave. Source: [7].

In an RDE, the detonation wave travels circumferentially around the annular detonation chamber, as depicted in Figure 2. The different regions of the flow field can be analyzed by unrolling the annular chamber into a 2-D image, as depicted in Figure 5, where the x-axis is the circumferential location and the y-axis is the axial location within the chamber. The detonation wave requires an approximate refresh height, H, of one to two cell heights, λ. As the detonation wave, region A, moves from left to right causing the oblique shockwave, B, to occur. Behind the shock wave is the induction zone which creates the temperature and pressure region necessary for the combustion to occur in the reaction zone. The region where the recently detonated products meet the previously detonated products, C, is known as the slip line. The non-detonated products expand in region D as they move towards the exit of the chamber. F displays an area where there are blocked injectors with possible reverse flow as the pressure from the detonation wave is greater

than the pressure pushing the fuel and oxidizer into the chamber. As the detonation wave moves away from the blocked injectors, the pressure from the detonation decreases and fuel and oxidizer begin to fill the chamber in zone G, where deflagration, E, occurs between the previously detonated products and fresh products entering the channel until being hit by the detonation wave again [5]. Because these shockwaves traverse axially and azimuthally away from the injector, they will eventually reach the chamber exit. The shockwaves cause large unsteady spikes in pressure and temperature, therefore determining a steady state average pressure in an RDE is not as straightforward as in a Brayton Cycle engine, where the flow field is more uniform. Additionally, many current diagnostic systems cannot survive the harsh environment within the flow field long enough to directly measure the total pressure within the chamber.
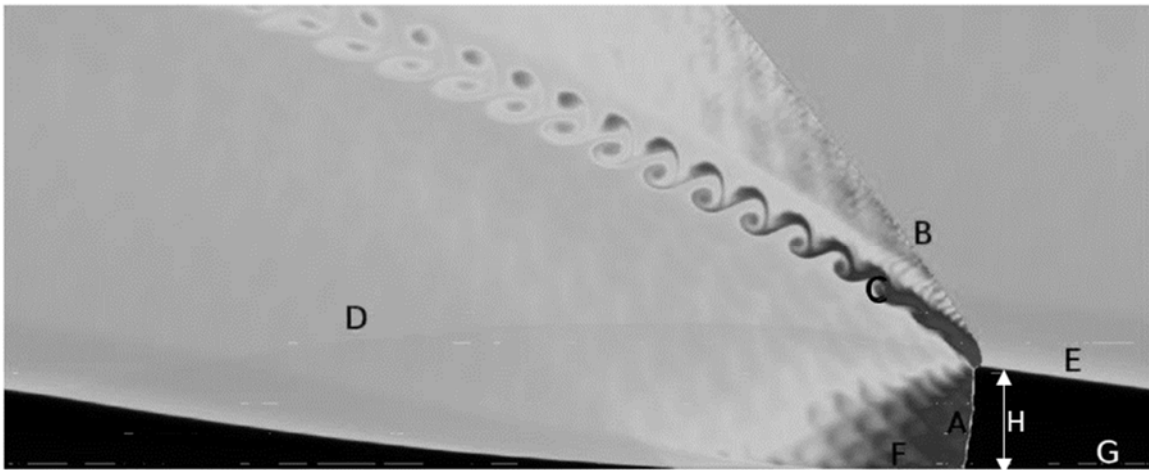
Figure 5.   Unrolled RDE Flow Field. Source: [5].

A main benefit of using an RDE over a traditional Brayton Cycle combustor is the ability to reduce the required size of an engine. The detonation cycle requires less compression as the initial shock wave greatly increases the pressure of the reactants. Additionally, the necessary length of the chamber greatly diminishes. In a rocket engine, the combustion chamber must be large enough to create complete combustion of the propellant [8]. The required chamber length of an RDE directly correlates to the detonation cell size, which for a hydrogen fuel, with a stochiometric mixture, is approximately 1.0 cm

at atmospheric pressure [3]. Therefore, the necessary chamber length and diameter of an RDE can likely be up to an order of magnitude smaller than that of a conventional engine. It can be shown that as long as a refresh height of at least 1λ is maintained, a detonation will likely propagate. This clearly is affected by how long the flow is allowed to reestablish the minimal refresh height and is a function of diameter, mass flowrate and cell size. The decreased size poses increased capabilities for rockets and missiles. The extra space could be used for more fuel and therefore longer-range missions. The characteristic pressure gain of the detonation cycle is an additional benefit to the engines, since an engine that had the same mass flow rate, same fuel type, same exit area, the thrust would be greater if the delivered total pressure is higher than a conventional constant pressure combustion process [8].

Though pressure gain across the combustor is a valuable capability of an RDE, this characteristic has not been evaluated historically for most of these engines. The idea of an RDE was first investigated in the 1950s by J.A. Nicholls [9] however, experimental studies of the engines lay dormant until 2004 where Wolanski, Fujiwara, and Mitsubishi applied for a patent on RDEs [10]. Even after 2004, most detonation engine efforts were geared towards understanding and characterizing PDEs. It was not until around 2009 that RDE experimentation became more common. Therefore, this relatively new technology has required several areas of investigation to include thrust performance of varying nozzles types [11], optical diagnostic of combustion efficiency internal and external to the combustor [12–13], flow field characterization [14] and computational modeling of RDE combustors [15].

B.   NAMING CONVENTION

For ramjets and other high-speed air breathing propulsion devices, a normalized naming convention for the thermal cycle has been implemented [16]. To remain consistent among airbreathing propulsion devices, the RDE community has adopted the same station labeling convention depicted in Figure 6 and annotated in Table 1. This convention will be used for the remainder of the paper. Locations of note are the differences between the 3.1 and 3.2 reference frames. The air inlet to the injector, 3.1, describes the minimum area

experienced by the air passing through the injector; whereas, 3.2 is the inside of the combustion chamber.
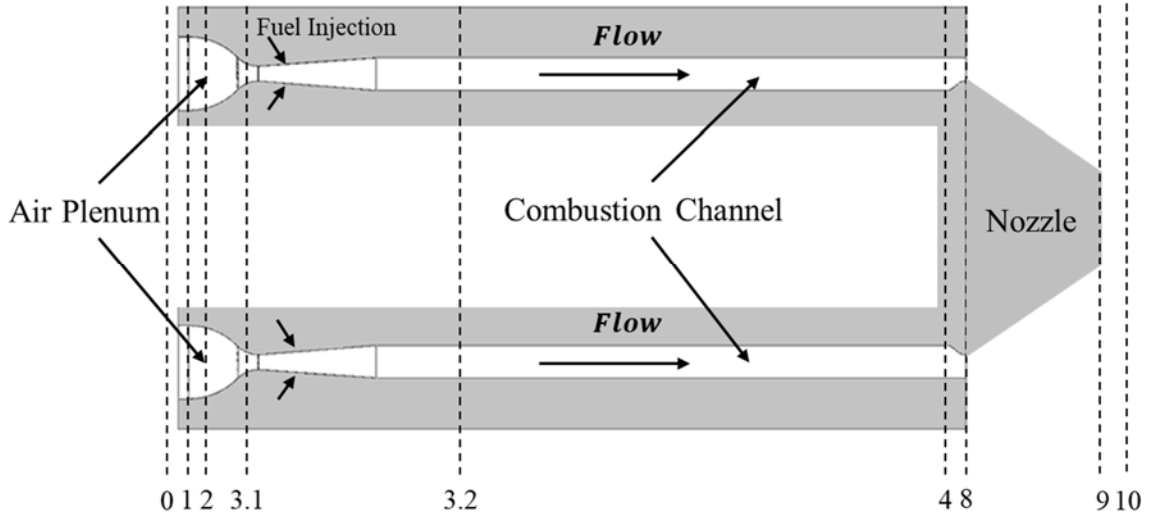
Figure 6.   Reference Locations in an RDE. Adapted from [16].

Table 1.   Reference Location Definitions for a Ramjet. Adapted from [16].

Location	Reference Value
0	Free Stream Air
1	End of Internal Compression
2	Air Plenum
3.1	Air Inlet Minimum Area
3.2	Combustor Chamber Area
4	Combustor Exit
8	Nozzle Throat
9	Nozzle Exit
10	Expanded Air

C.   EFFECTIVE PRESSURE

RDEs are pressure gain combustion devices, therefore the total pressure entering the combustion entrance should be lower than the total pressure at the exit of the combustor. For typical Brayton cycle engines, there is a total pressure loss in the combustor, due to the thermodynamics of the deflagration process, flame holders, and heat loss. From steady state analysis or direct measurement of a Brayton cycle engine, determining the static pressure is a simple steady state pressure transducer measurement or calculation from the engine's exhaust velocity with isentropic flow equations used to convert to stagnation pressure [17]; however, an RDE chamber pressure is time varying with extreme fluctuation in both temperature and pressure as the detonation wave rotates around the annular chamber. Current instrumentation cannot survive inside an RDE or adequately determine the chamber flow stagnation pressure. Therefore, the effective available pressure (EAP) represents the effective total pressure from time averaged static values that are more easily obtained.

The definition of EAP is "the flow stagnation pressure which is representative of a flows ability to do work or provide thrust" [18]. The methodology for determining EAP was first posed by Kaemming and Paxson [6]. The thrust equation is typically broken down into a momentum thrust term and a pressure thrust term; in order to only investigate the thrust produced by the combustor itself and not include uncertainties from nozzle effects. An additional term—base drag—is included in this equation as seen in Equation 1 and visualized in Figure 7:

$$F_g = \dot{m}V_8 + (P_8 - P_0)A_8 + F_{BaseDrag} \qquad (1)$$
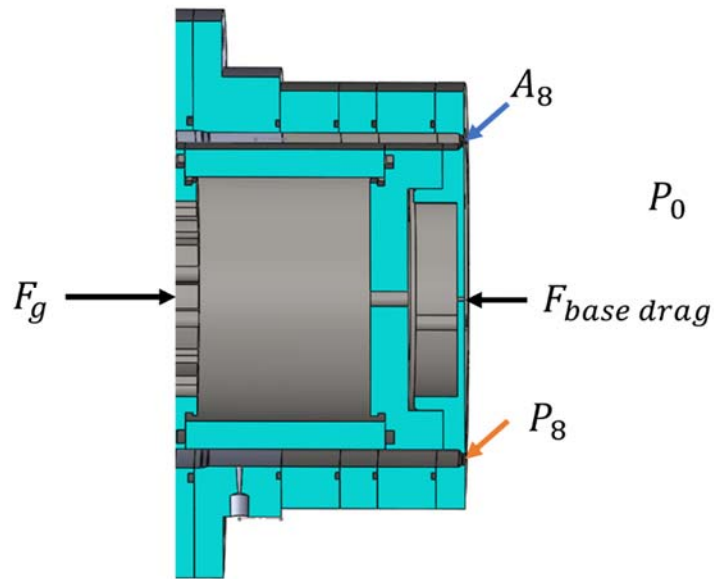
Figure 7. RDE Control Volume

In order to remove nozzle effects, a simple choked exit plane (bluff body) with a converging throat but no supersonic nozzle divergence was implemented, as displayed in Figure 8. This plate is described as a base drag bluff body. The force acting on the bluff body produced by the flow field must be modeled or experimentally considered while calculating the thrust of the engine to ensure the thrust value evaluated was solely produced by the combustor conditions. Experimentally, base drag can be approximated with several static pressure measurements on the inner and outer body of the exit plane. Figure 9 displays the base drag bluff body configuration when viewed from the aft end of the combustor with flow directed out of the page.
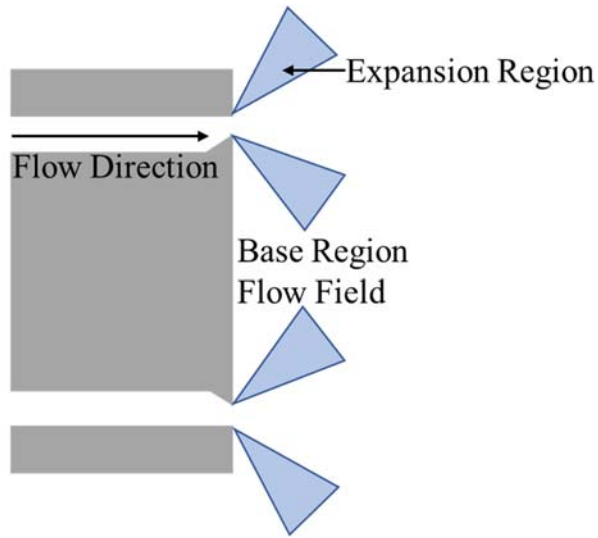
Figure 8. Base Drag Bluff Body Design to Remove Nozzle Effects on EAP
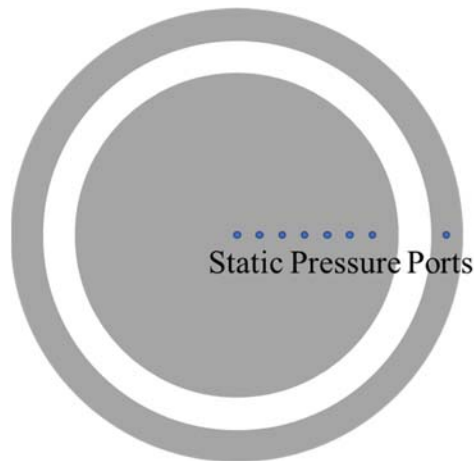
Figure 9. Example Static Pressure Readings for Base Drag Measurement

The force caused by the base drag is simply the pressure experienced on the bluff body and outer ring multiplied by the area over which that pressure is sensed; therefore, the more pressure ports spaced radially on the surfaces, the higher the fidelity of the base drag model. By rearranging the momentum thrust equation, Equation 1, as a function of Mach number, Equation 2 is derived:

$$F_g = P_8 A_8 (1 + \gamma M_8^2) - P_0 A_8 + P_{base} A_{base} \tag{2}$$

All values of Equation 2 can be experimentally measured, except for the exit pressure, p_8, and the exit Mach condition. The gross thrust force can be measured by the thrust stand. The ambient pressure term is accounted for by utilizing gauge pressure transducers, the ratio of specific heats, γ, is assumed as 1.24 for the combustion products as per CEA, and the Mach number at the exit is assumed at sonic or one as per reference [6], which indicates that the exit Mach value likely stays between 0.9 and 1.1 for the majority of the runs. The assumption of M_8 can be shown in reference [6] to yield the most conservative results. Equation 3 displays the known values on the right side of the equation and unknown values on the left.

$$\widetilde{P_8} = \frac{F_g + P_0 A_8 - P_{base} A_{base}}{(1 + \gamma M_8^2) A_8} \tag{3}$$

The exit pressure, $\widetilde{P_8}$ is a derived effective static pressure value at the throat of the nozzle. A tilde is used to annotate the value, P_8, is not experimentally measured but driven from other measurable values. In order to analyze total pressure, isentropic relations were implemented to switch to an effective available total pressure or EAP, as seen in Equation 4.

$$EAP = \widetilde{P_{T8}} = \widetilde{P_8} \left(\frac{\gamma + 1}{2}\right)^{\frac{\gamma}{\gamma-1}} \tag{4}$$

Therefore, EAP can be determined for an RDE by measuring thrust, the machined bluff body exit area, and static pressures acting on the backpressure bluff body and outer ring. In order to look at the pressure gain over the combustor, Equation 5 is utilized:

$$\% P_{gain} = \frac{EAP_{abs} - P_{T2}}{P_{T2}} * 100\% \tag{5}$$

The pressure gain, as a percent, is the percent difference between the absolute total pressure in the RDE and the measured pressure at the inlet of the combustor, or the air plenum pressure.

III.   EXPERIMENTAL SETUP

A.   RDE SPECIFICATION

The RDE utilized in this experiment was located in Test Cell #2 at the Naval Postgraduate School's Rocket Propulsion Combustion Laboratory as depicted in Figure 10. The RDE operates on air as the oxidizer and gaseous hydrogen as the fuel. Air was supplied from two high pressure storage banks, at pressures up to 6.8 MPa, to the test cell through three manual and pneumatic ball valves as well as a TESCOM 26–2065T24A273 regulator to set and control the flow and pressure entering the test cell. After going through a final manual insolation ball valve, air traveled through 12x1.27cm (0.5in) tubes and 12 sonic chokes, to meter the mass flowrate of the air, between the manifold and plenum. Each choke had a 4.37mm (0.172 in) diameter orifice and was calibrated using a NIST-traceable metering venturi.

Hydrogen was supplied via two banks of gaseous hydrogen six packs, which are manually isolated by two ball valves. At full capacity the hydrogen tanks supply 13.8MPa (2000 psig) and were usually switched out at 6.20 MPa (900 psig). Once in the test cell a final manual ball valve is opened leaving one pneumatic valve to control hydrogen flow to the rig. A hand regulator located in the test cell was used to set the desired pressure of supplied hydrogen to the engine due to its stability over an actively tuned regulator. Similar to the air system, the hydrogen was choked by a 5.15mm (0.203in) choke, and metered prior to entering 4x1.27cm (0.5in) lines to the RDE plenum. The fuel and air are mixed by an injector with a jet in cross flow configuration. A small pulse detonator initiates a pre-detonation wave within the RDE, which propagates a detonation wave circumferentially around the annular chamber. The complete air and fuel lines schematic is displayed in Figure 11.

Figure 10.   RDE Experimental Setup

For every test case, gases were controlled by two separate LABVIEW files by two operators. The test engineer commands the air operator to achieve a specific air set pressure. The electronically controlled air regulator is set to the desired pressure and the air operator waits for the test engineer to confirm air flow delivery. Once air is flowing through the RDE, the test engineer starts fuel and ignition LABVIEW sequence. Fuel begins flowing through the rig and once steady-state has been achieved, the pre-detonation initiates the RDE. A trigger was sent to the high-speed camera to record wave speed and the number of waves. A secondary DAQ is manually triggered immediately prior to ignition, and records base drag and chamber pressures. Each run is designated to run for 1–2 seconds. Since there was not active cooling and some materials in the test hardware

have low melting temperatures, the engine was not designed to run for extended periods of time. After the designated run time has elapsed, the fuel was shut off with an electronically controlled pneumatic ball valve. Air flow was then manually shut off utilizing the air LABVIEW program. If the rig required immediate hardware changes, air would be run through the RDE for a few more seconds to cool the rig via convection. If there was a safety concern during the run, both the test engineer and the air operator have an emergency E-stop button in which they can press and end the run immediately.
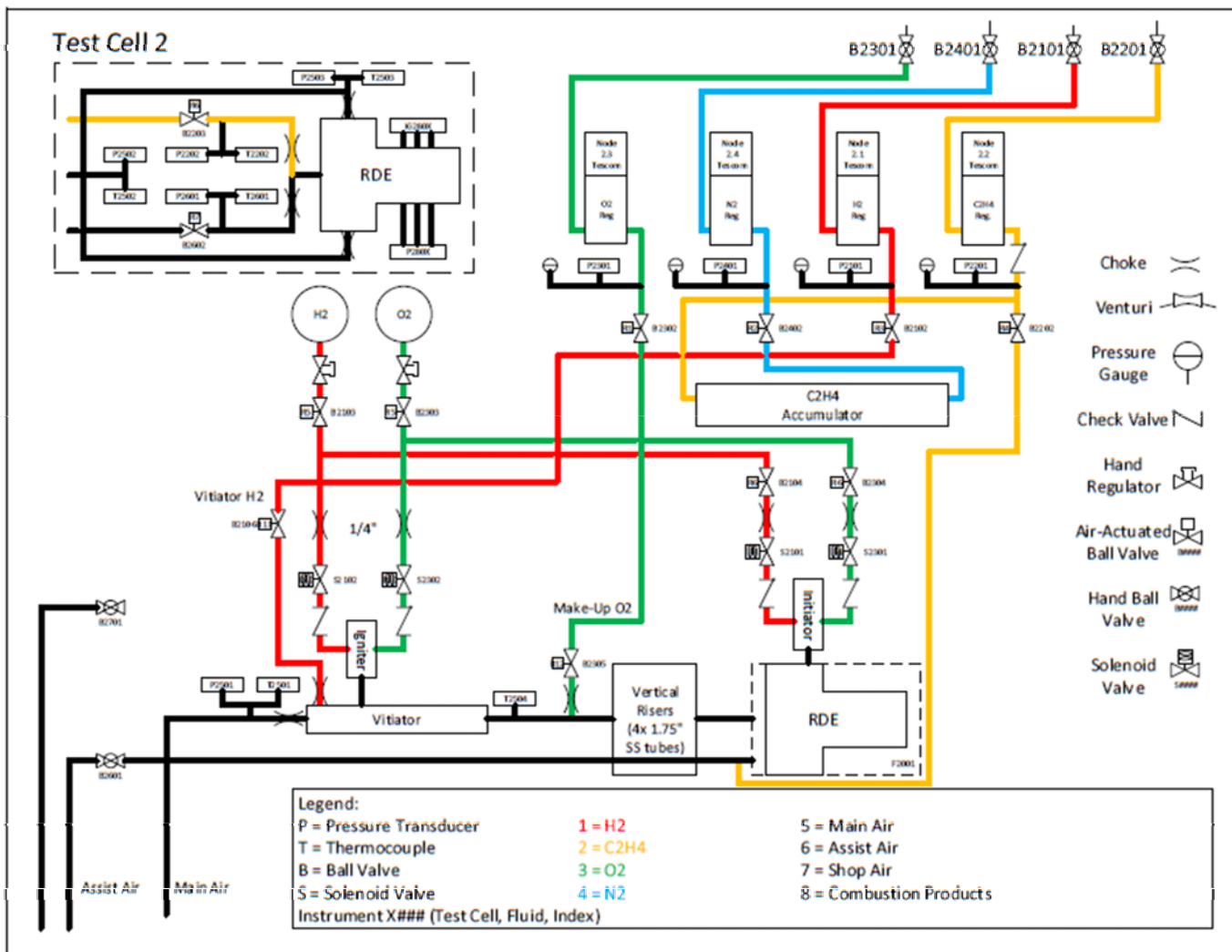
Figure 11.   TC2 Fuel and Air Lines Schematic

B.   DATA ACQUISITION

The two DAQs used were denoted as the main DAQ and mobile DAQ. Main DAQ received the vital values necessary to characterize the conditions of each run: mass flowrate of air and fuel, equivalence ratio, air and fuel supply pressures, and thrust. The mobile DAQ was used to record data for this specific experiment: base drag pressures, chamber pressures and air plenum pressure.

The main DAQ consists of a National Instruments (NI) PXIe-1062Q Chassis with DAQ blocks installed to receive and transfer different data sets. A NI PXIe-6225 M-series multifunction DAQ installed received pressure data readings from a NI BNC-2110 Block. A NI PXI-6221 M-series multifunction DAQ received all thrust stand and thermocouple data via a 16-bit connector to three NI-SCXI-1314 universal strain gauge modules. The thrust stand utilized was designed specifically for TC2 by Pacific Press Company. There are 18 load cells capable of decoupling axial loading of the RDE. After calibrations, the absolute uncertainty in the axial thrust is 0.1% of 2224 N (500 lbf) or 2.22 N (0.5 lbf). The main DAQ setup and thrust stand in TC2 are depicted in Figure 12 and Figure 13.
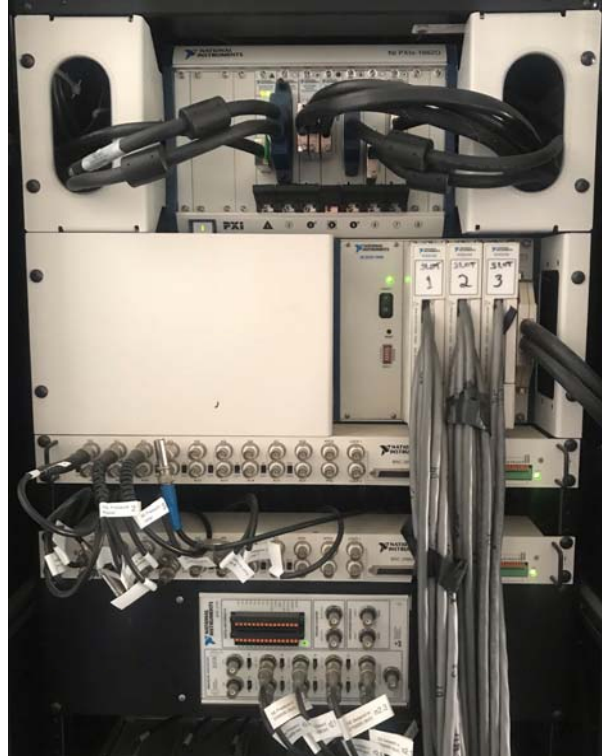
Figure 12.   Main DAQ setup

Figure 13.   Thrust Stand

The mobile DAQ is a NI PXIe-1082 Chassis with a NI PXIe-6363 X-series multifunction DAQ installed, as depicted in Figure 14.

Figure 14.   Mobile DAQ Setup

The PXIe-6363 X-series DAQ has 32 single ended or 16 differential, 16 bit analog to digital converter channels. With 16-bit precision and a ±10 V operating range, the DAQ is capable of resolving voltage changes down to 0.9 mV; therefore, the DAQ provided greater precision than could be resolved by the transducers. For this experiment, only one of the two ports were used and connected to a NI BNC-2111 which connected the DAQ to the BNC wires in the test cell. The fully instrumented NI BNC-2111 block is depicted in Figure 15.

Figure 15.   NI BNC-2111 Instrumented with TC2 BNC Wires

The BNC wires ran through the floor of the command room, down a transit pipe, through the concrete blast wall, and to TC2. The BNCs run directly into a BNC to 4-pin connector box with a voltage supply for the transducers. The four pin data and power lines were routed to a transducer bank located behind the engine. Both the converter box and transducer bank are displayed in Figure 16.

Figure 16.   BNC to 4-Pin Converter (left) and Transducer Bank (right)

C.   CTAP LINES

Capillary Tube Averaged Pressure (CTAP) consist of 1.6 mm (0.0625 in) diameter stainless steel tube that range from 0.33 m to 2 m long. Because the diameter is so small in comparison to the length of the tube, the viscous effects damp the unsteady pressure to achieve a constant time averaged pressure value [19]. Figure 17 depicts the comparison of a CTAP calculated pressure to that of an Infinite Tube Pressure (ITP) which are more closely coupled to a combustion chamber. The red line depicting the large spikes in the pressure seen in an RDE whereas the black line stays at a constant time averaged pressure. Though CTAP lines provide a steady state value, the losses at the entrance to the tube are not well characterized; therefore, CTAPs provide a steady state approximation of an unsteady value but do not provide an exact steady state static pressure.
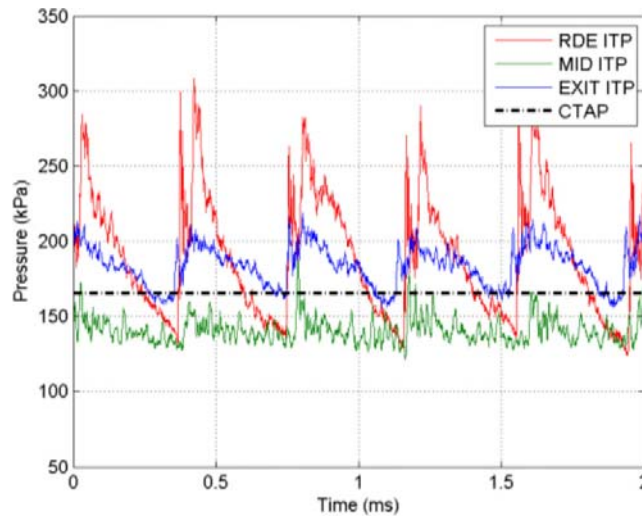
Figure 17.   Comparison of CTAP Pressure Measurements. Source: [19].

The length of a CTAP tube effects the pressure received by the transducer. If the tube is too short, the viscous losses are unable to adequately damp the transient response. In order to determine the ideal length of CTAP, an annular outer body ring was implemented on the chamber of the RDE with eight CTAP ports at the same axial location. The annular ring with CTAP locations is displayed in Figure 18 and the length of the CTAP lines are located in Table 2. One end of the tube is located in a static configuration on the

combustion chamber wall while the other end it attached to a pressure transducer. Because all ports were at the same axial location in the chamber, the pressures produced by the transducers should be equal. Figure 19 depicts the results of one of the RDE tests with the annular CTAP ring implemented after applying a baseline correction.
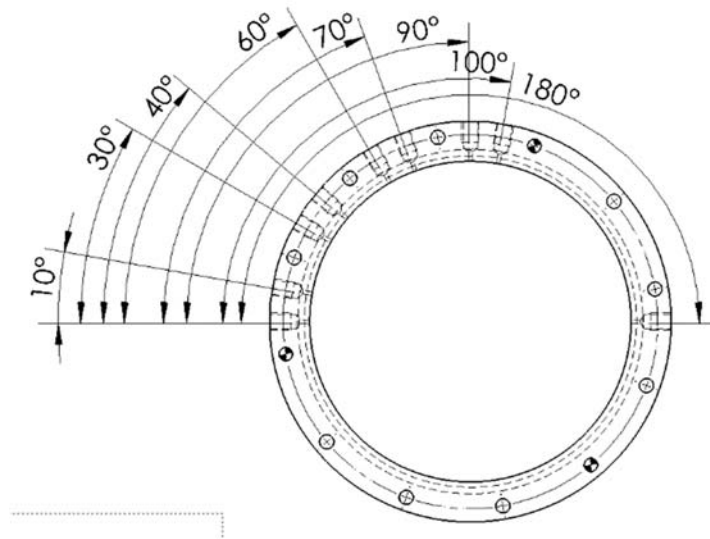
Figure 18.   CTAP Combustor Ring used for CTAP Length Comparison

Table 2.   CTAP Lengths and Locations on Ring

Probe	Reference Angle (⁰)	Length (m)	Length (in)
CTAP 1	0	0.30	12
CTAP 2	10	0.46	18
CTAP 3	30	0.61	24
CTAP 4	40	0.91	36
CTAP 5	60	1.22	48
CTAP 6	70	1.52	60
CTAP 7	90	1.83	72
CTAP 8	100	2.13	84
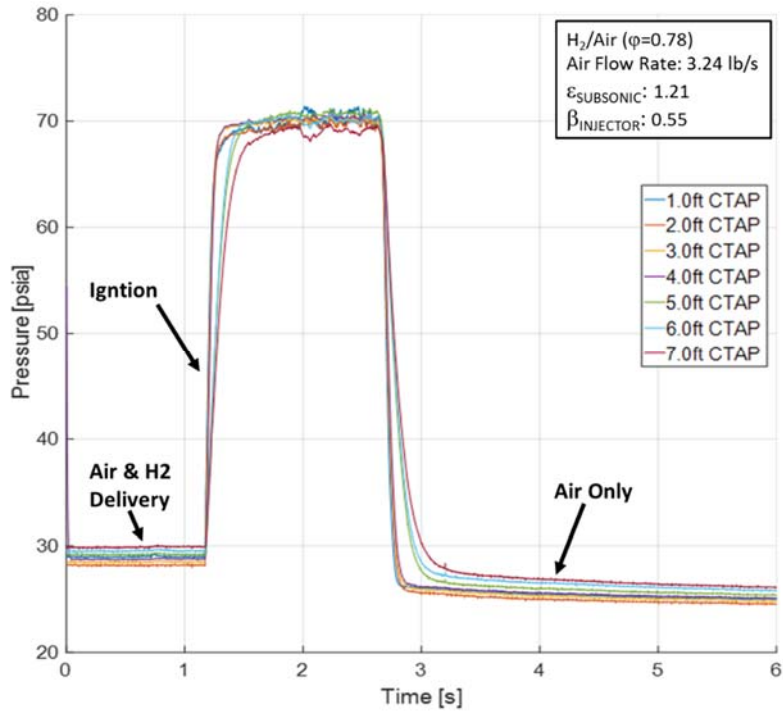
Figure 19.   CTAP Length Comparison for Pressures in Combustion
Chamber. Source: [20].

Figure 19 displays the three regions of an RDE test at the NPS RPCL; data collection begins when both the air and fuel are up to pressure and flowing through the rig. Next the ignitor starts the detonation propagation and continues until fuel is shut off. After, air only flows through the rig until it is also shut off. Upon ignition, the shorter CTAP lines respond quicker to achieve the pressure of the chamber, whereas the larger volume in the 1.52, 1.82, 2.13 m (5, 6, and 7 ft) resulted in a larger time delay to reach steady state. The 0.30 m and 2.13 m (1 ft and 7 ft) CTAP display temporal details instead of remaining steady state, therefore additional investigation into the flow and expected pressures of CTAPs is necessary for better characterization. The 0.3 m (1 ft) line was not used for the remainder of testing despite having a quick rise time, as it possessed more inherent unsteadiness and was not believed to adequately protect the transducer from the harsh environment cause by the detonation wave. All lines achieve a similar constant value; however due to the rise time, 0.61-1.22m (2-4 ft) CTAP lines were used for the remainder of RDE pressure measurements.

D. BASE DRAG MEASUREMENT

The base drag bluff body was designed with a converging throat but without nozzle divergence. Ten CTAP lines were spaced radially outward at 0.70 cm (0.275 in) increments to measure the base drag on the center body of the RDE. Each CTAP line was cut to 0.69 m (27 in). Figure 20 displays the face view of the bluff body with radial spacing measurements located in Table 3. Since the center of the test hardware remained open, CTAP lines were able to run directly through the middle of the RDE without affecting the engine. The outer body base drag measurements were taken through two CTAP ports going to CTAP lines on the outside of the RDE as depicted in Figure 21.
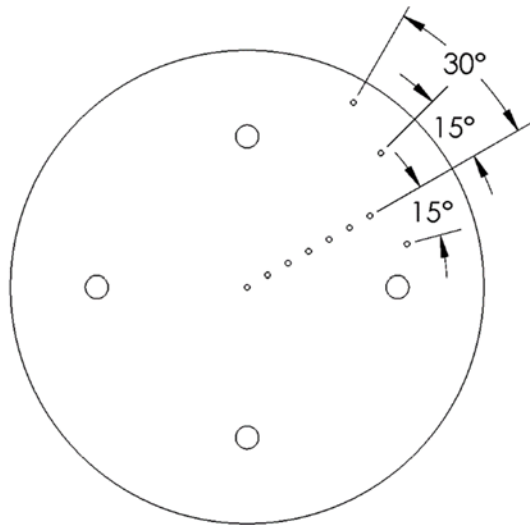
Figure 20.   Depiction of Base Drag Bluff Body CTAP Locations
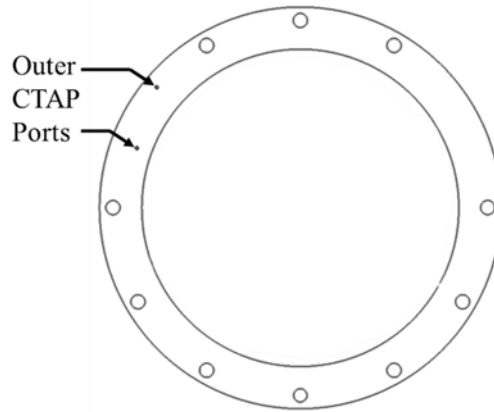
Figure 21.   Depiction of Outer Body Base Drag CTAP Locations

Table 3.   CTAP on Base Drag Bluff Body Radial Location

CTAP	Radius (cm)	Radius (in)	Angle (º)
CTAP 1	0	0	0
CTAP 2	0.70	0.275	0
CTAP 3	1.40	0.550	0
CTAP 4	2.10	0.825	0
CTAP 5	2.80	1.100	0
CTAP 6	3.50	1.375	0
CTAP 7	4.19	1.650	0
CTAP 8	4.89	1.925	-15
CTAP 9	5.59	2.200	15
CTAP 10	6.29	2.475	30
CTAP 11	8.26	3.250	0
CTAP 12	8.89	3.500	15

E.   PRESSURE MEASUREMENTS

Calculations of EAP and pressure gain rely heavily on the capability and calibration of the transducers utilized. For this paper, Omega PX 600 series, PX613 and PX603,

transducers were used for the majority of the pressure measurements. For the base drag, 15&VAC and 0&VAC transducers were used on the outer nine CTAP ports; where 15&VAC means the transducer was capable of reading 204.7kPa (15psig) to vacuum and 0&VAC could read 101.3kPa (0psig) to vacuum. The other transducers used on the inner three CTAP ports of the bluff body were originally Omega PX 140 differential transducers. These transducers have two ports to be able to measure the differential pressure between two regions. By leaving one of the ports open to ambient pressure, the transducers were able to measure from 101.3kPa (0psig) to vacuum. Images of both the PX613 and PX140 transducers are located in Figure 22.

Figure 22.   PX613 Transducer (right), and PX140 Transducer (left).
Source: [21].

Due to apparent noise in the transducer circuitry, the three PX140 transducers were later replaced by PX 613 15&VAC transducers. For chamber pressure CTAP, air plenum pressure, detonation channel and static chamber pressure readings, PX 613 1480.3kPa (200psig) transducers were installed. Accuracy of the PX 600 transducers were 0.4% and 0.75% for the PX 140 [21]. Therefore, for the 15&VAC transducers, the error was ±0.41 kPa (0.06 psi) since the pressure reading is a differential pressure. For the 0&VAC transducers the error was ±0.41 kPa (0.06 psi), for the 1480.3 kPa transducers the error was ±5.92 kPa (0.80 psi), and for the PX140 transducers the error was ± 0.78 kPa (0.11 psi). It was possible for the shockwaves and high temperatures, though suppressed by the CTAP

lines, to degrade the signal output of the transducers over several runs, therefore baselines were taken every day to check the functionality of all transducers. All 200psig transducers were calibrated utilizing pressurized nitrogen and a well characterized mechanical pressure gauge, Heise Pressure Calibrator.

Since the voltage produced by the transducer has a linear correlation to the pressure, a slope and intercept for all transducers were used to convert the raw voltage data to pressure data. Vacuum transducers, which were straight from the factory, utilized factory calibration values. Baseline ambient pressure values were taken before and after testing to ensure transducer results remained valid for the entirety of testing. The baseline ambient pressures were also subtracted from pressure reading to ensure ambient pressure changes were normalized to compare several runs over multiple days of testing.

F.   GEOMETRY DESIGN

Kaemming and Paxson discuss how the geometry of the RDE affects the EAP and pressure gain. Through use of computational analysis of an RDE, they compared pressure gain to the ratio of the exit area to the chamber area ($A_8/A_{3.2}$) as well as the ratio of the air inlet to the chamber area ($A_{3.1}/A_{3.2}$) to show EAP pressure gain trends. Figure 23 displays the analysis produced by Kaemming and Paxson. For their study, they used an air breathing, hydrogen fuel design with a mass flowrate of 1.0 kg/s and an equivalence ratio of 1, or a stochiometric condition [6]. Complete combustion and no heat loss was also assumed for the figure, although it is discussed in detail in reference [6].
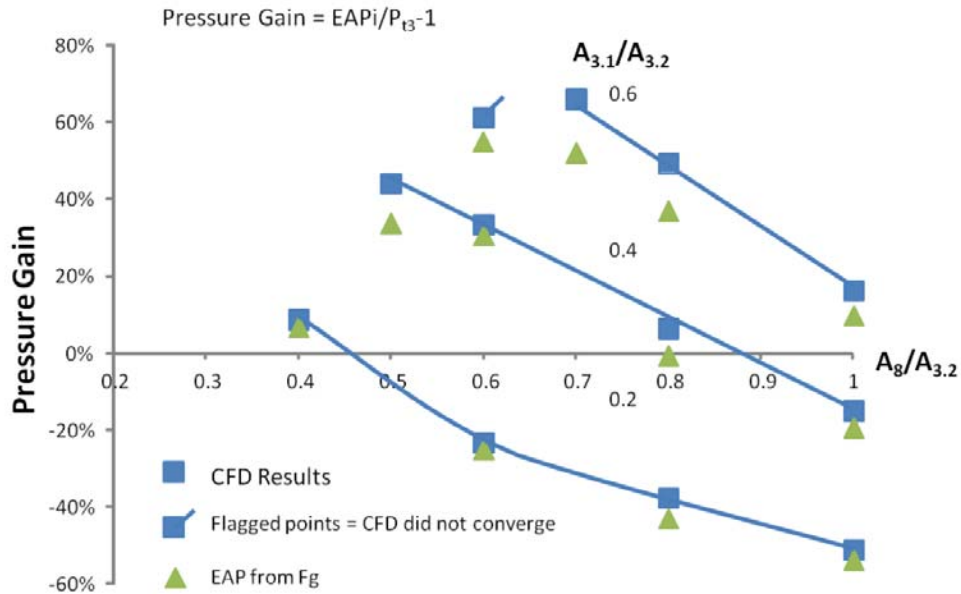
Figure 23. Analysis of Geometry Effects on Pressure Gain. Source: [6].

By utilizing nondimensionalized values, this plot can be compared to any airbreathing hydrogen fueled RDE. The modeling utilized by Kaemming and Paxson displays values for an ideal combustor; therefore, for injectors with poor mixing of the fuel and oxidizer, the pressure gain will be lower than the values displayed due to incomplete combustion. In order to validate the results of experimentally calculating EAP and pressure gain for an RDE, several different geometries were utilized. The exit area, A_8, was modified to produce three different Mach numbers in the chamber: 0.58, 0.45, and 0.30 while the chamber area, $A_{3.2}$, remained constant. The three area ratios, $A_8/A_{3.2}$, were 0.83, 0.68, and 0.48 respectively. Therefore, three points would be placed in a single line on Figure 23 to validate the results. As $A_8/A_{3.2}$ decreases, the pressure gain of the combustor increases. By decreasing the exit area, the Mach number in the combustor decreases therefore the velocity in the chamber also decreases; a slower velocity creates an increase in static pressure in the chamber thus increasing the pressure gain across the combustor.

Because the base drag bluff body was costly and difficult to manufacture, different converging exit outer body plates were implemented on the design to vary the exit area. Figure 24 displays the SOLIDWORKS rendering of the RDE with the 0.45M plate

30

installed. There were two CTAP ports located on the downstream side of the plate to measure backpressure on the outer body of the rig. Figure 24 also displays the cross-sectional view of the inside of the rig beginning at the injector plane. Two CTAP ports were located inside the chamber to compare the EAP measurements to a physical CTAP static pressure in the chamber. The expected result from Kaemming and Paxson's analysis displays that as the exit area becomes less restrictive the amount of pressure gain decreases.
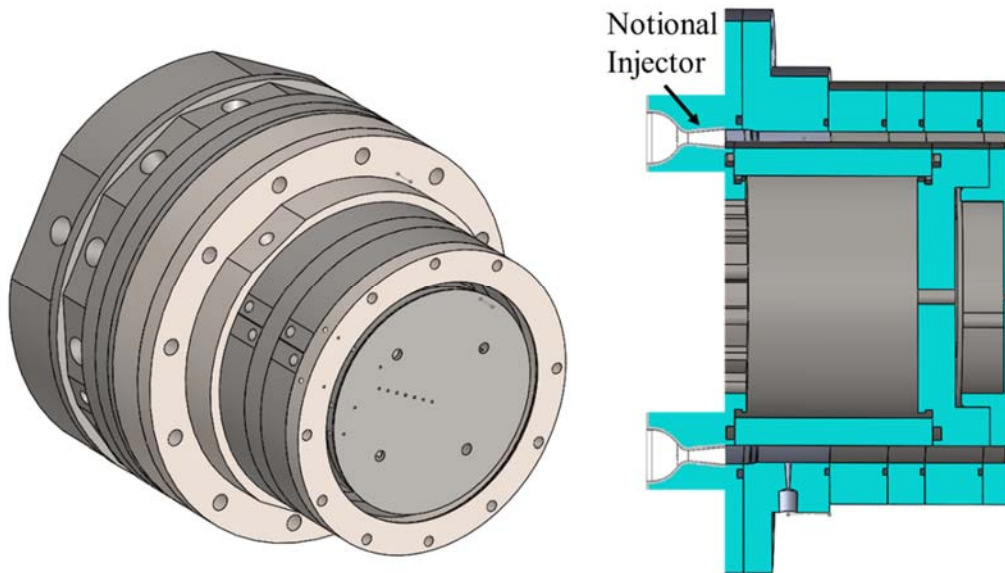
Figure 24.   SOLIDWORKS Rendering (left) and Cross Section (right)
of RDE with 0.45 Exit Mach Plate

The next part to the experiment was to modify the air inlet to produce different lines, $A_{3.1}/A_{3.2}$. A simplistic air inlet scheme is depicted in Figure 25 to provide a visual description of the area. As the air inlet area is decreased, the pressure losses across the restriction increase, thus driving the overall pressure gain across the combustor down.
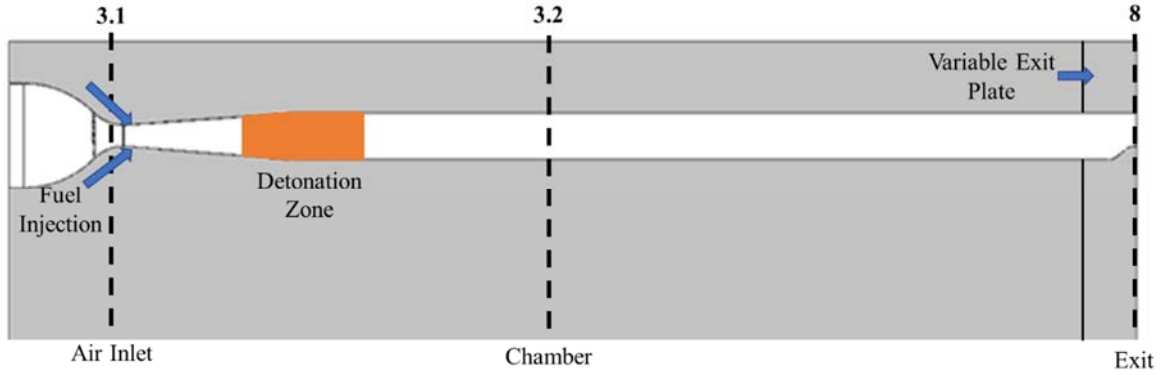
Figure 25.   Notional Schematic of Air and Fuel Inlet to Chamber

Although Figure 25 represents a generic and simplified axial fuel RDE system, the Figure captures the regions were the geometry was modified. Spacer plates were added upstream of the injector on both the inner and outer body of the rig to increase the inlet area ratio. Two different spacer plate thicknesses were machined, a 0.508 cm (0.2 in) and 0.762 cm (0.3 in) thick aluminum flange, resulting in area ratios of 0.50 and 0.57 respectively. Without the flanges the air inlet ratio was 0.30. Because the inlet area produced by the hardware was difficult to directly measure without large uncertainties, these ratios were calculated utilizing choked air flow across the injector. The conservation of mass dictates the equation for mass flow choking in an ideal compressible gas, Equation 6 [17]. If the flow is chocked across a minimum area restriction, the Mach number is set at 1.0, or sonic. Therefore, by ensuring the flow was choked between the air manifold and inlet to the injector, as well as from the inlet to the chamber, Equation 6 can be simplified. Flow is considered choked if the pressure ratio of absolute downstream pressure over absolute upstream pressure is less than the critical value of 0.528.

$$\dot{m} = C_d \frac{A p_t}{\sqrt{T_t}} \sqrt{\frac{\gamma}{R}} M \left(1 + \frac{\gamma - 1}{2} M^2\right)^{-\frac{\gamma+1}{2(\gamma-1)}} \tag{6}$$

Where T_T is assumed at 288.7 K, γ is 1.4, R is 287.05 Jkg^{-1}K^{-1}, and C_d was measured to be 0.91 for the choke between the air manifold and air inlet and 1.0 between the inlet at the chamber. Utilizing the air manifold pressure and minimum area of the choke, a mass flow rate was computed. Since the mass flow rate across the entire system should remain

constant, the mass flowrate value is set equal to Equation 6 for the air injector inlet; therefore, the minimum area for the air inject inlet can be determined. This area is an effective area, therefore if there are small eddies or restriction in the flow, the computed area accounts for them. Equation 6 was also used to measure air and fuel mass flowrates. A known C_d choke was inserted into air and fuel lines; since there is a sonic condition at the throat, a simple pressure transducer can be used to determine mass flowrate.

As shown in Figure 23, by increasing the inlet area, the pressure gain should also increase. Since both the exit area and air inlet area are compared to the combustor chamber entrance, conclusions can be made on the correlation between the two values. Each directly affect the static pressure in the chamber. If the chamber static pressure increases, the overall pressure gain of the system also increases. If the air inlet area, $A_{3.1}$, is small in relation to the nozzle exit area, A_8, there are large pressure losses across the inlet due to choking over the entire RDE cycle [6].

For all geometries, equivalence ratio, ϕ, and air mass flowrate, $\dot{m}_{air}$, were varied to show the effect on EAP. Equivalence ratio sweeps from 0.6 to 1.0 were taken at mass flowrates of 0.5 and 1.0 kg/s. As well as a φ of 1.0 at 0.75 kg/s to provide a constant φ, varying mass flowrate curve for each geometry. For the least restrictive back pressure plate, the 0.58 Mach plate, higher mass flowrates would be necessary to produce the chamber conditions to support detonations; therefore, mass flow rate was varied at 1.0, 1.25, and 1.5 kg/s at a constant φ of 1.0.

THIS PAGE INTENTIONALLY LEFT BLANK

IV. RESULTS AND ANALYSIS

A. RAW DATA ANALYSIS

Two computers with LABVIEW were used independently to control the facility air and RDE test sequence. The duration of each test was set to one second as this enabled enough time to reach stable thrust and pressure values but minimize fuel usage and stress on the hardware. The desired air pressure was set first, and delivered to the engine. Then, the second control computer started the RDE test sequence, opening fuel control valves and initiating the pre-detonation. Due to the number of data logging channels required to measure the base drag, a secondary DAQ chassis controlled from a third computer was necessary. The low speed data acquisition system could only store 10 sec of data at a sampling rate of 1000 times per second, therefore, the data acquisition was triggered about 1 sec prior to ignition for each run to capture the fuel and air steady state pressure and the air only steady state pressure after the run. A Photron FASTCAM SA-Z camera was used to image the combustion chamber from the aft end of the RDE rig. This camera provided insight into the type of combustion—deflagration or detonation—occurring in the chamber as well as an optical method to determine detonation wave speed.

All transducers, PX 600 series and PX 140, output 1–5 V and 1–6 V, respectively to the DAQ. A calibration for each transducer was applied during data processing. Baseline pressure values were used to normalize the transducer voltages to determine and remove initial ambient before testing occurred each day. Figure 26 displays the translation from raw voltages to pressure values.
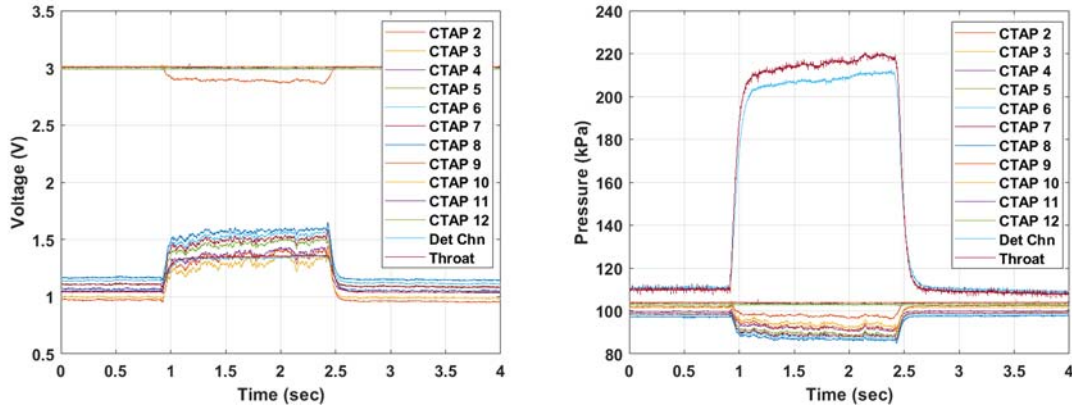
Figure 26. Typical Voltage (Left) and Pressure (Right) Values of Base
Drag and Chamber Measurements

Most of the pressure transducers output voltages near 1V while at ambient pressure. The four voltages near 3V are the 15&VAC PX613 transducers. For the 0&VAC and PX140 differential transducers, if the voltage is increased, a vacuum is being pulled on the system; alternatively, for the PX613 200psig transducers, if the voltage is increased the pressure increases. The 15&VAC transducers start in the middle, at 3V, and if there is a vacuum being pulled the voltage decreases and if there is a positive pressure the voltage increases. Two CTAP lines were placed inside the chamber of the RDE to measure a static steady state pressure near the detonation region in the channel and downstream near the nozzle entrance. The downstream chamber pressures were compared to the EAP values to investigate the use of CTAP lines to experimentally determine pressure gain readings.

The labeling of the CTAP lines for the base drag calculations follow the references described in Figure 20 where CTAP 1 displays the inner most reading on base drag bluff body, CTAP 10 displays the outermost port on the bluff body, and CTAP 11 and 12 are the inner and outer ports, respectively, located on the exit plate outer body. Transducer calibrations and types for each CTAP location are located in Table 4.

Table 4.   Transducer Calibrations

CTAP Location	Transducer Type	Slope (kPa/V)	Intercept (kPa)
CTAP 2	0&VAC PX613	-25.34	126.69
CTAP 3	0&VAC PX613	-25.34	126.69
CTAP 4	0&VAC PX613	-25.34	126.69
CTAP 5	0&VAC PX613	-25.34	126.69
CTAP 6	0&VAC PX613	-25.34	126.69
CTAP 7	0&VAC PX613	-25.34	126.69
CTAP 8	0&VAC PX613	-25.34	126.69
CTAP 9	15&VAC PX613	51.71	-53.78
CTAP 10	15&VAC PX613	51.71	-53.78
CTAP 11	15&VAC PX613	51.71	-53.78
CTAP 12	15&Vac PX613	51.71	-53.78

The bluff body and outer body plate into regions based off the CTAP port locations, as displayed in Figure 27 to determine the areas in which the different CTAP's pressures were acting upon.
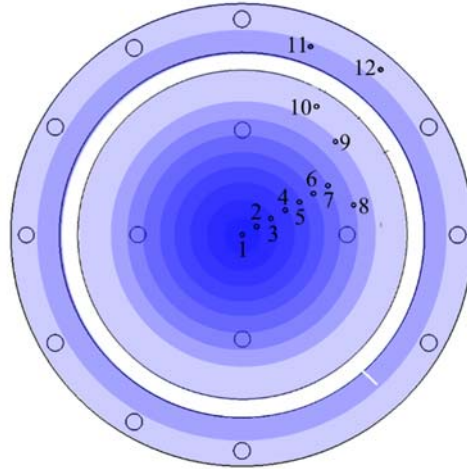
Figure 27.   Area Regions on Bluff Body and Outer Body for Base Drag
Measurements with CTAPs Numbered

The outer three regions are broken up differently from the inner eight. The inner eight regions were constructed from the area between concentric circles with an inner radius of the previous CTAP port and an outer radius of the current CTAP port. The last region on the truncated nozzle is from CTAP 9 to the edge of the bluff body as there is not a port at the very edge of the nozzle. Because the outer body nozzle only had two CTAP ports, the midpoint between the inner radius and outer radius of the plate was the line of demarcation between the two regions. If the base drag regions were broken down directly between each CTAP location, the change in base drag force was around ±3 N or a ±0.2% pressure gain effect, therefore the interpolation schemed described above was used for all testing.

CTAP 1 was not used for any calculation because the area region breakdown described in Figure 16 would have the CTAP 1 area equal to zero. Focusing solely on the base drag pressure measurements, the two values measured with PX140 transducers, CTAP 2 and 3, were extremely noisy in comparison to the PX613. Figure 28 displays the same data set with and without the two PX140 transducers present.
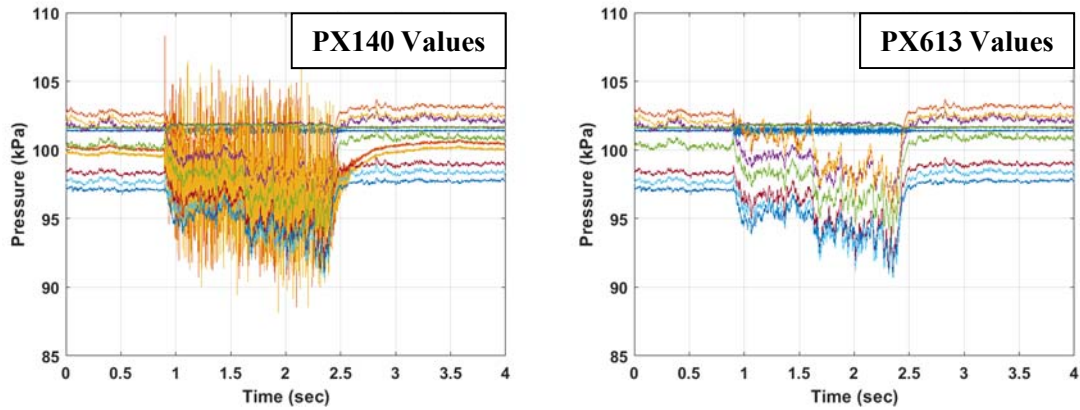
Figure 28.   Base Drag Pressure Values with PX140 (left) and without PX140 (right)

Due to the low signal to noise, these transducers were moved to the center ports, CTAP 2 and 3, to have the smallest area regions and effect on the overall base drag force. Later in the testing, new PX613 transducers were purchased and implemented to remove the noise problem completely. Figure 29 displays a typical pressure result with all PX613 transducers implemented for base drag calculations.
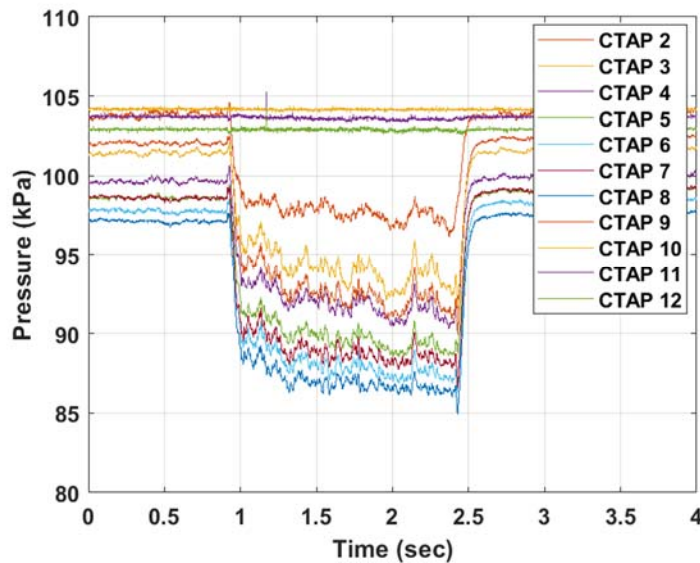
Figure 29.   Typical Base Drag Pressures for All PX613 Transducers

The results from the PX613 transducers produce smaller standard deviations in time averaged data and therefore were used for the majority of the runs. CTAP values were time averaged over 200 data points, 0.2 seconds, towards the end of the run. For example, for Figure 29, the CTAP pressures were averaged from 1.9 to 2.1 seconds. Each averaged pressure value was multiplied by its corresponding area region and summed to produce the base drag force acting on the engine. Assuming the exit Mach is sonic and a ratio of specific heat of 1.24, for combustion products, EAP is calculated utilizing Equations 3 and 4. The complete test matrix is located in Appendix A as there were 70 tests of the RDE to produce data points for the different exit areas and inlet gaps.

B.   EXAMPLE PERFORMANCE CALCULATION

The following example calculation was for a mass flowrate of 0.78 kg/s and an equivalence ratio of 1.00, or stochiometric. The rig was configured with the 5.08mm (0.2 in) aluminum spacer plate upstream of the injector opening the air inlet ratio, $A_{3.1}/A_{3.2}$, to 0.50. Additionally, the most restrictive back pressurization plate, 0.48 $A_8/A_{3.2}$ was installed. This example is of a nominal run and the calculations were implemented for the entire data set to determine the EAP and pressure gain of the combustor over various configurations and conditions.

1.   Base Drag Measurement

The base drag measurement utilized 11 CTAP ports attached to the base drag bluff body and outer body to determine the pressure acting on the body. Each pressure measurement was multiplied by the specified area it acted over. The main DAQ used for controlling the RDE did not have enough open data ports for the 11 base drag CTAP measurements and two chamber measurements, therefore a small mobile DAQ was installed and used separately to acquire this data. Figure 30 displays the raw voltage data for this run recorded on the mobile DAQ as well as the resulting base drag pressures once the calibrations were applied.
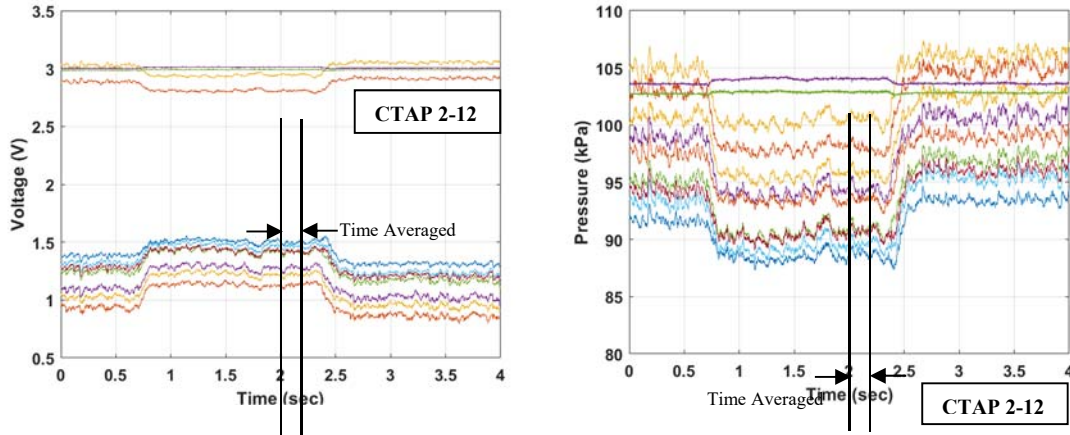
Figure 30.   Raw Data (left) and Pressure Data (right) for $\dot{m}_{air}$=0.78 and φ=1.0

In order to determine a time averaged pressure measurement for the base drag readings, 200 data points were averaged near the end of each run. The pressure curves displayed in Figure 30 were averaged from 2.0 to 2.2 seconds and the time averaged pressure values are located in Table 5.

Table 5.   Base Drag Measurements

CTAP LOCATION	2	3	4	5	6	7	8	9	10	11	12
BASE DRAG PRESSURE (kPa)	98.4	96.0	94.4	90.9	89.6	90.6	88.6	93.5	100.6	104.1	98.4
CORRECTED GAUGE PRESSURE (kPa)	-6.60	-7.57	-8.37	-11.7	-11.2	-11.3	-11.3	-10.2	-7.8	0.11	-0.02
EFFECTIVE AREA (cm²)	1.5	4.6	7.7	10.7	13.8	16.9	19.9	23.0	55.2	53.9	54.2
BASE DRAG FORCE (N)	-1.0	-3.5	-6.4	-12.6	-15.4	-19.0	-22.5	-23.5	-43.0	0.6	-0.1

Each pressure was then multiplied by the effective area to calculate the force on the base drag bluff body. Since the base drag bluff body is always subject to atmospheric pressure, gauge pressure was used for the remainder of the analysis for that force component. The transducers read ambient pressure during the baseline, the values were corrected to ensure the results were consistent and normalized. The corrected pressure row

in Table 5 displays the same pressures located in the row above but corrected for baseline and converted to a gauge pressure.

Utilizing the CTAP radial locations, displayed in Table 3, the areas were determined and multiplied by the corrected pressures to determine the regional base drag measurements. All the regional forces were then summed to produce a total base drag acting on the aft end of the engine. For this example, the force of base drag came out to be -146.4 N. Because the flow was pulling a vacuum on the bluff body, the thrust stand was displaying a lower thrust than what was achieved by solely the momentum exiting the combustor.

2. Main DAQ Data

The main DAQ of TC2 recorded valuable information necessary to classify each run: mass flowrates, equivalence ratio, air plenum pressure, and thrust. Since the mass flowrate for both the fuel and air were known, the equivalence ratio could be determined utilizing air and hydrogen's mass fractions. Figure 31 displays the run data for the 0.78 kg/s, φ of 1.0 test condition necessary to calculate EAP and pressure gain.
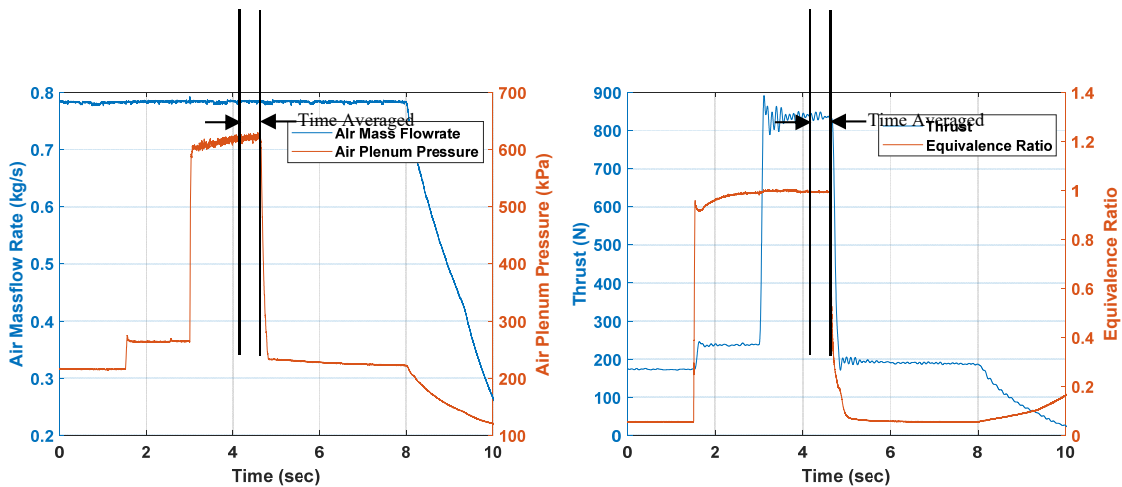
Figure 31. Plots of Main DAQ Data to Analyze EAP

The data for the run depicted in Figure 31 was taken from 4.1 to 4.3 seconds. Timing for the two DAQs is different because the main DAQ was triggered by the ignition sequence and the mobile DAQ was manually triggered. To mitigate error, both data sets

were averaged towards the end of the run where values were most steady. Air mass flowrate remained relatively constant over the entire run; at 8 seconds air was shut off and the air pressure reduced back down to ambient, decreasing the mass flowrate. The initial spike in air plenum pressure and thrust was caused by the opening of the fuel line at approximately 1.5 seconds. Air plenum pressure increases by approximately 30 kPa (4.35 psi) during the run however towards the end of the run, the pressure leveled out. Over the averaged time period, air plenum pressure only deviated 2 kPa (0.3 psi). Equivalence ratio achieved a steady value shortly after opening the fuel line and by the end of the run, thrust also leveled out. The time averaged values recorded from the main DAQ are located in Table 6.

Table 6.   DAQ Time Averaged Data

Air Mass Flowrate (kg/s)	Equivalence Ratio	Air Plenum Pressure (kPa)	Thrust (N)
0.78	1.00	620	841

3.   Effective Available Pressure

After the data from both the main and mobile DAQs were time averaged, the EAP for the combustor was be calculated. Utilizing Equation 3, a derived pressure at the throat can be calculated as shown in Equation 7.

$$\widetilde{P_8} = \frac{F_g + P_0 A_8 - P_{base} A_{base}}{(1 + \gamma M_8^2) A_8} = \frac{840.5\ (N) + 101352.9\ (Pa) * 0.001702\ (m^2) + 146.4\ (N)}{(1 + 1.24 * 1^2) * 0.001702\ (m^2)} \quad (7)$$

$\widetilde{P_8}$ was determined to be 304.1 kPa (43.9 psia). Utilizing isentropic relations for an ideal gas the static $\widetilde{P_8}$ value was converted to a total or stagnation pressure as given by Equation 8.

$$EAP = \widetilde{P_{T8}} = \widetilde{P_8}\left(\frac{\gamma + 1}{2}\right)^{\frac{\gamma}{\gamma - 1}} = 304107(Pa) * \left(\frac{1.24 + 1}{2}\right)^{\frac{1.24}{1.24 - 1}} \quad (8)$$

EAP was determined to be 546.1 kPa (78.9 psia). By comparing EAP to absolute air plenum pressure, an effective pressure gain percentage can be determined across the combustor, as given by Equation 5 and calculated in Equation 9.

$$\% \, P_{gain} = \frac{EAP_{abs} - P_{plenum_{abs}}}{P_{plenum_{abs}}} * 100\% = \frac{546159 \, (Pa) - 620100 \, (Pa)}{620100} * 100\% \quad (9)$$

The percent pressure gain was determined to be -11.9%; therefore, there is a 11.9% loss in the effective global total pressure .

C.   ERROR CALCULATION

Error bars provide validity and understanding of the data displayed in the analysis section. The calculation of EAP, as displayed in Equations 3 and 4, is a function of thrust, base drag, exit area and ratio of specific heats. Breaking these down into experimentally measured values, the possible sources of error are the thrust stand, the pressure transducers and the measured areas of hardware. All experimental measurements were averaged over a 0.2 sec, 200 data points, range towards the end of the run. Since all measured values had reached near constant state, the averages were viewed as a singular data point. Additionally, the analog to digital converter used, described in section Figure 11, had higher sensitivity than the pressure and thrust stand were capable of producing, and therefore was considered to have negligible effect on the measured data. The calibrated thrust stand error was ± 2.2 N as specified by the manufacturer. The PX600 series transducers have a specified 0.4% accuracy; both the 15&VAC and 0&VAC transducers were used in the base drag measurement and had a ±0.4 kPa error. The air plenum pressure transducer was a PX600 series with a 1379 kPa (200 psig) range, therefore its accuracy was ±5.7 kPa. The exit area and base drag area were calculated off of part designs with a ±0.0508 mm (0.002 in) diameter tolerance. The assumed value of specific heats was taken a from CEA calculation with a range of equivalence ratios and was assumed at 1.24 for the mixture conditions. For various runs calculated in CEA, the ratio of specific heats varied between 1.22 and 1.26.This parameter was determined to have marginal effects on error with only a ±0.6% error on the EAP or ±0.2% error on the pressure gain for the example described in IV.B.

The EAP error calculation was broken down into a thrust and a base drag error before being combined for total pressure gain error. The thrust stand axial thrust error is ±2.2 N. For the base drag, the error was a combination of the 11 transducer pressures and area calculations. This error was determined by utilizing the worst-case area for both the base drag bluff body and the outer flange area: the product of the pressure accuracies and the sum of the base drag area and the maximum tolerance. The maximum total base drag error was determined to be ±10.4 N.

Determining whether the area or the pressure accuracy drives the total error is important for future iterations of this work. Considering run 6 on 19-Apr-19, the base drag was 281 N. If the pressure measurements were assumed to have incurred no error, and the only error came from the hardware area measurements, the incurred error on the base drag would be ±0.16 N. If the area measurements were held constant with no error and the only error occurred from the pressure transducers' accuracy, the error on the base drag would be ±10.2 N. Therefore, the error on the base drag measurement is more sensitive due to the accuracy of the transducers than the area measurements.

The sensitivity to the exit area measurement was also calculated for run 6 on 19-Apr-19. Utilizing the machine tolerance for both the inner diameter and outer diameter of the exit area to investigate the minimum and maximum exit area within the machine tolerances, The EAP calculation had an error of ±10.2 kPa and the overall pressure gain had an error of ±1.7 %. Therefore, EAP and pressure gain are very sensitive to any alterations in exit area, physical or perceived by the flow.

Utilizing the combination of Equations 3 and 4, the maximum EAP error was computed as displayed in Equation 10:

$$Error_{EAP} = \frac{Error_{F_g} - Error_{base\ drag}}{(1 + \gamma M_8^2)A_8}\left(\frac{\gamma + 1}{2}\right)^{\frac{\gamma}{\gamma - 1}} \tag{10}$$

where γ is 1.24, M_8 is 1.0, and A_8 is determined by the different exit flanges area minus the maximum tolerance. The EAP errors for the 0.3M, 0.45M, and 0.58M configurations were ±6.0 kPa, ±4.3 kPa, and ±3.5 kPa respectively. For pressure gain calculations, the error must be calculated separately for each run as a ratio of worst case pressures plus their

respective errors. The lower mass flowrate runs produced lower pressures therefore the error on the pressure calculations had a greater effect on the overall pressure gain of the system. For the entire test campaign, the pressure error was between ±6.0% with the average value being ±1.9% on pressure gain. The pressure gain error for each test case was calculated and is provided as error bars on each plot.

D. ANALYSIS

For each run, the base drag, EAP, and pressure gain were calculated. The four variables changed to affect these values were the mass flowrate, equivalence ratio, exit area, and air inlet area. Figure 32 displays a constant air mass flowrate of 1.0 kg/s at a constant air inlet ratio but varying exit area ratio.
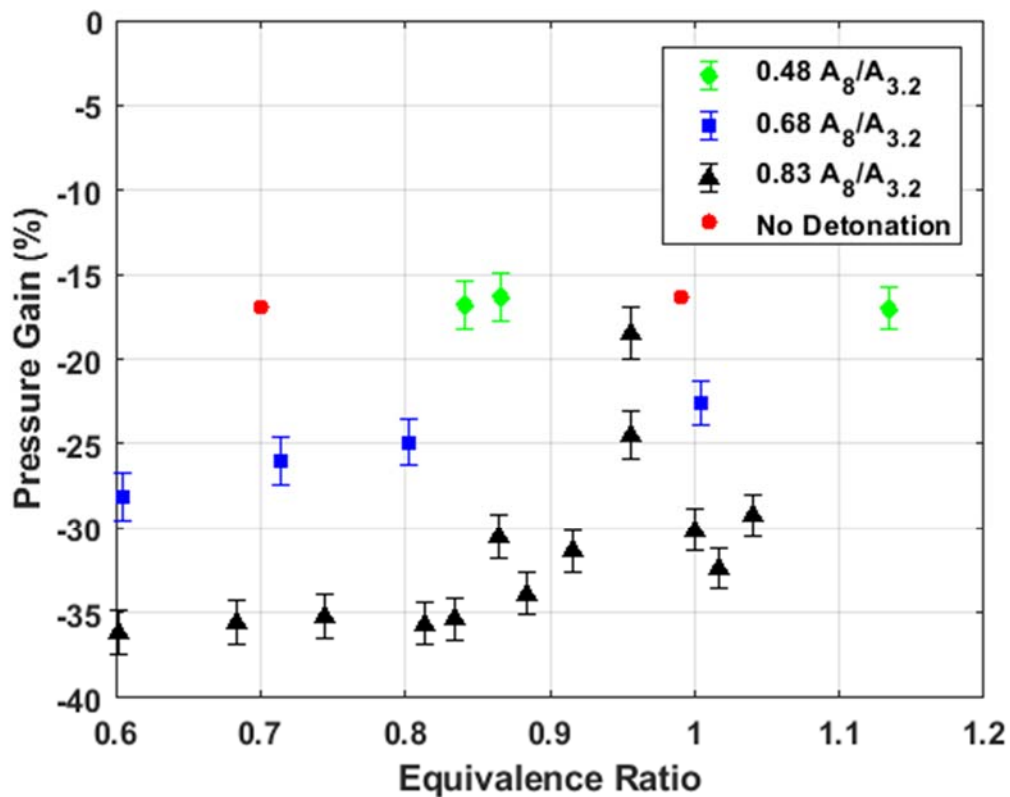
Figure 32.   Constant Mass Flowrate of 1.0 kg/s for 0.30 $A_{3.1}/A_{3.2}$

For Figure 32 air mass flowrates greater than 0.95 kg/s and less than 1.05 kg/s were considered to be constant at 1.0 kg/s. As equivalence ratio approaches stochiometric, a φ of 1.0, the pressure gain increases. When the equivalence ratio is low, the engine is running lean—there is more oxidizer flowing through the system than necessary to combust all the fuel—effecting both the heat release and cell size of the detonation. Figure 33 displays how low equivalence ratios affect different fuels. For hydrogen fuel, the smallest cell size occurs around stochiometric and as the mixture becomes leaner, the cell size quickly grows. The larger cell sizes increase the difficulty to achieve detonation waves in small scale devices and decreases the number of wave fronts produced in the RDE. Therefore, the highest performance of the RDE, for a given air inlet and exit ratio, should occur near an equivalence ratio of 1.0 which is supported by Figure 32.
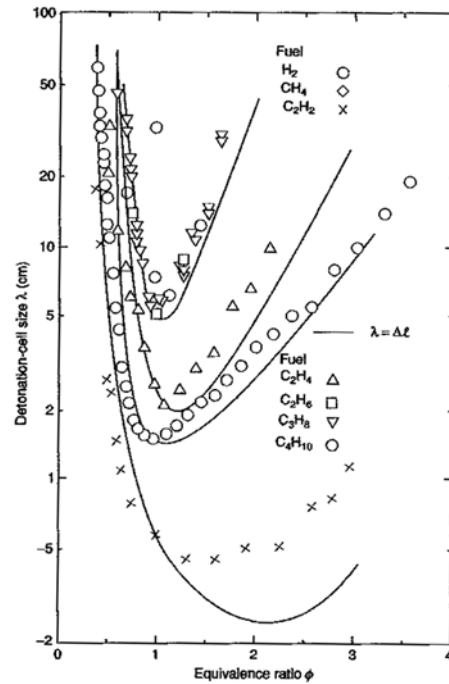
Figure 33.   Effect of Equivalence Ratio on Cell Size. Source: [3].

An exit area of 0.83 corresponds to a chamber Mach number of 0.58 and is the least restrictive exit used for this experiment. The least restrictive exit has the largest chamber Mach number and the greatest velocity in the channel. With a greater velocity, more of the

total pressure component is in the form of dynamic pressure, thus decreasing the static pressure in the detonation channel. Detonation waves primarily process the static pressure; therefore, a lower static pressure creates a smaller jump condition of the detonation wave. Additionally, as the velocity in the chamber increases, the detonation wave is restricted in its ability to impart additional momentum to the fluid, because fluid in a constant area channel is constrained to subsonic velocities. Therefore, a higher dynamic pressure component prior to the detonation wave leads to a smaller increase in final dynamic pressure and lower performance increase. With the higher velocity fluid, fuel mixing also decreases causing another degradation to overall combustor performance. If the chamber pressure decreases, so does the overall pressure gain across the device. If the exit area becomes more restrictive, the chamber Mach number in the chamber also decreases. The static pressure in the chamber increases before the detonation wave causing a larger jump condition, thus improving pressure gain. At some point, the refresh rate, the rate at which the fuel and oxidizer are able to refill the detonation zone, becomes too small and the operability of the engine decreases. For the 0.48 $A_8/A_{3.2}$, the engine had difficulty producing stable one wave propagation. If the detonation wave was not propagating circumferentially, axial pulsing occurred. The fuel would enter into the channel, combust, and send a compression wave upstream towards the injector, blocking the injectors momentarily. Once the pressure wave had passed, the channel would refill with fuel and oxidizer then combust again. Though this is a deflagration event, the process can be assumed as nearly constant volume due to the rate at which it occurs, therefore the global pressure losses from these non-detonation runs was similar to that of a detonation. In summary, as equivalence ratio approaches stochiometric, the pressure gain increases. Furthermore, as the exit area decreases, there are fewer pressure losses but also a smaller detonation operability range.

While keeping air mass flowrate constant, the air inlet ratio was also changed independently. Figure 34 depicts the 0.68 $A_8/A_{3.2}$ exit area ratio for varying air inlet ratios. The three ratios that were used were 0.30, 0.50, and 0.57 $A_{3.1}/A_{3.2}$.
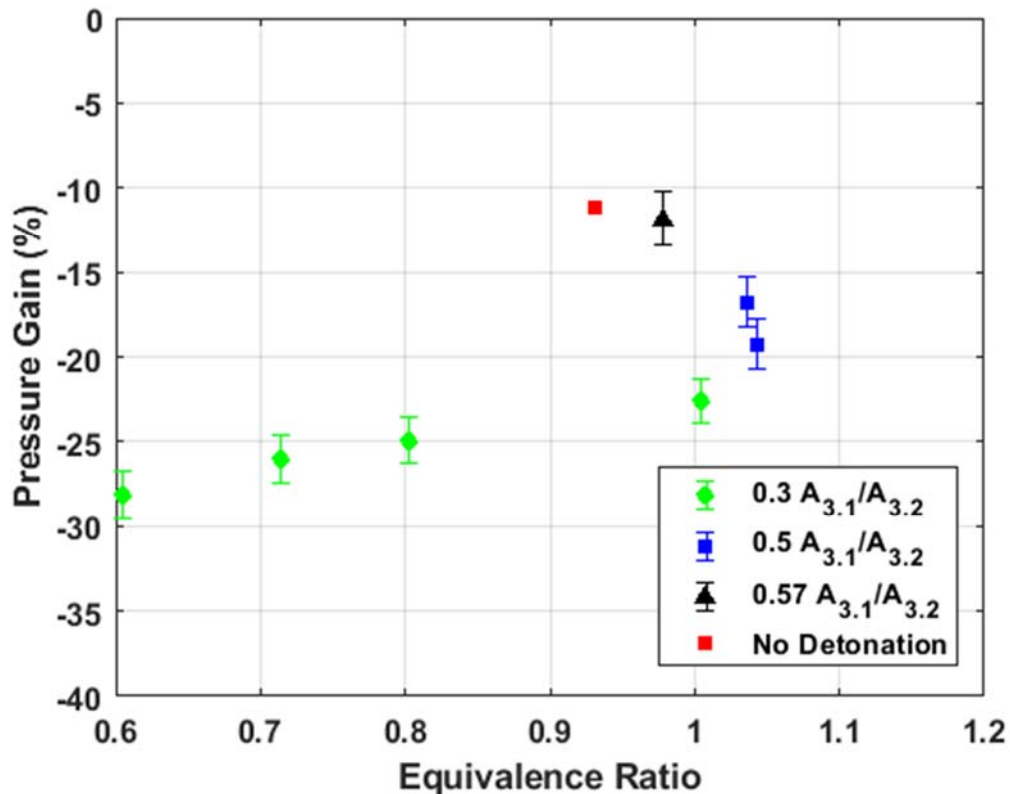
Figure 34.   Constant Mass Flowrate of 1.0 kg/s for 0.68 $A_8/A_{3.2}$

From Figure 34, as the air inlet ratio increases, the pressure gain also increases. With a large air inlet, the velocity of the flow is slower through the inlet, therefore less of the pressure is transformed to dynamic pressure; in other words, the static pressure is higher. For example, if a mass flowrate of 10 kg/s was desired through a 1 cm versus a 5 cm diameter restriction, the pressure driving the fluid through the smaller diameter would have to be far greater than the pressure to drive the fluid in the pipe. Less of the pressure is lost to the friction and edges of the restriction whereas the small restriction will have large viscous losses. These pressure losses are a part of the total combustor process, therefore by increasing the air inlet area the combustor, the overall pressure gain will also improve. Likewise, if the air inlet area is smaller, the fluid has a smaller restriction to fit through causing increased pressure losses across the restriction and decreased pressure gain. Therefore, Figure 34 displays as the equivalence ratio approaches 1.0 the pressure gain increases.

The next variable examined during the experiments was air mass flowrate. While keeping the mixture at a stochiometric condition, the mass flowrate was varied for a constant air inlet area ratio and a constant exit area ratio. Figure 35 displays the constant equivalence ratio with a constant air inlet area ratio.

For varying mass flowrate, the results are far less conclusive. Increasing mass flowrate did not substantially affect the pressure gain. Although thrust increases with more mass flowrate, the equivalence ratio remains constant. The separation between the 0.68 and 0.48 exit area ratios' pressure gain values is less obvious for this data set. This can be partly accounted for by the air inlet ratio. Because the largest air inlet ratio is utilized, the smallest exit area restriction may have been at too slow of a velocity in the chamber for a detonation to be sustained.
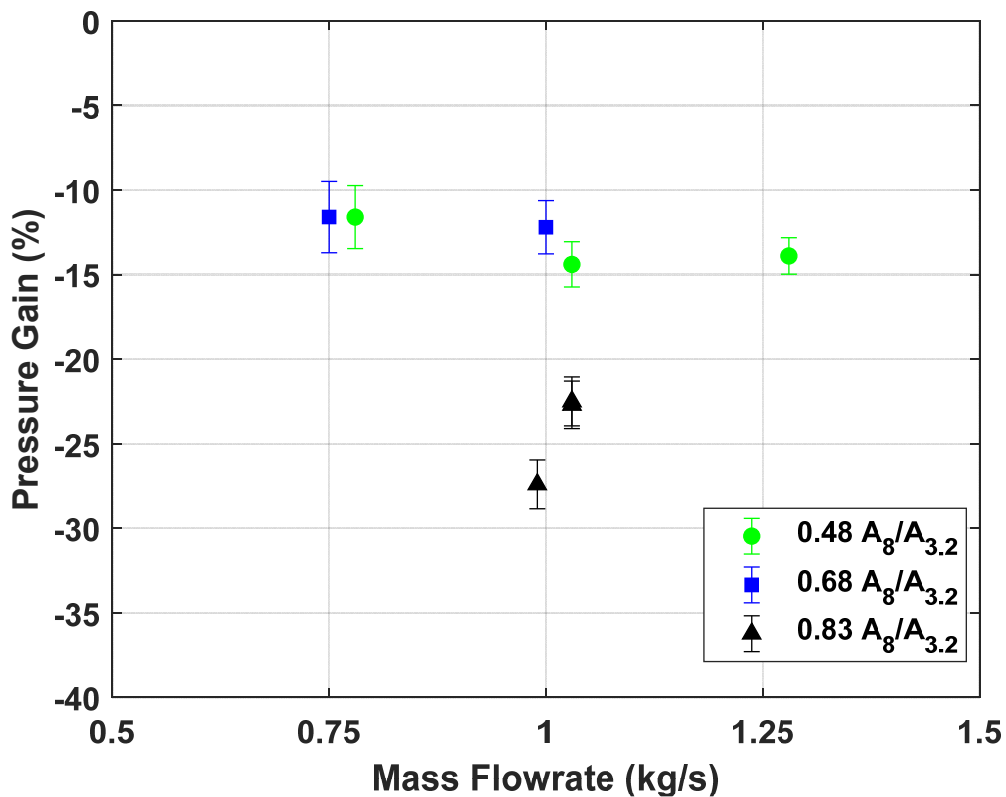
Figure 35.   Constant Equivalence Ratio of 1.0 for 0.57 $A_{3.1}/A_{3.2}$

Alternatively, when exit area is held constant at 0.68 $A_8/A_{3.2}$, and the air inlet area ratio is varied, EAP pressure gain is shown to increase. This trend is shown in Figure 36.. However, pressure gain still remains constant over varying mass flowrates.
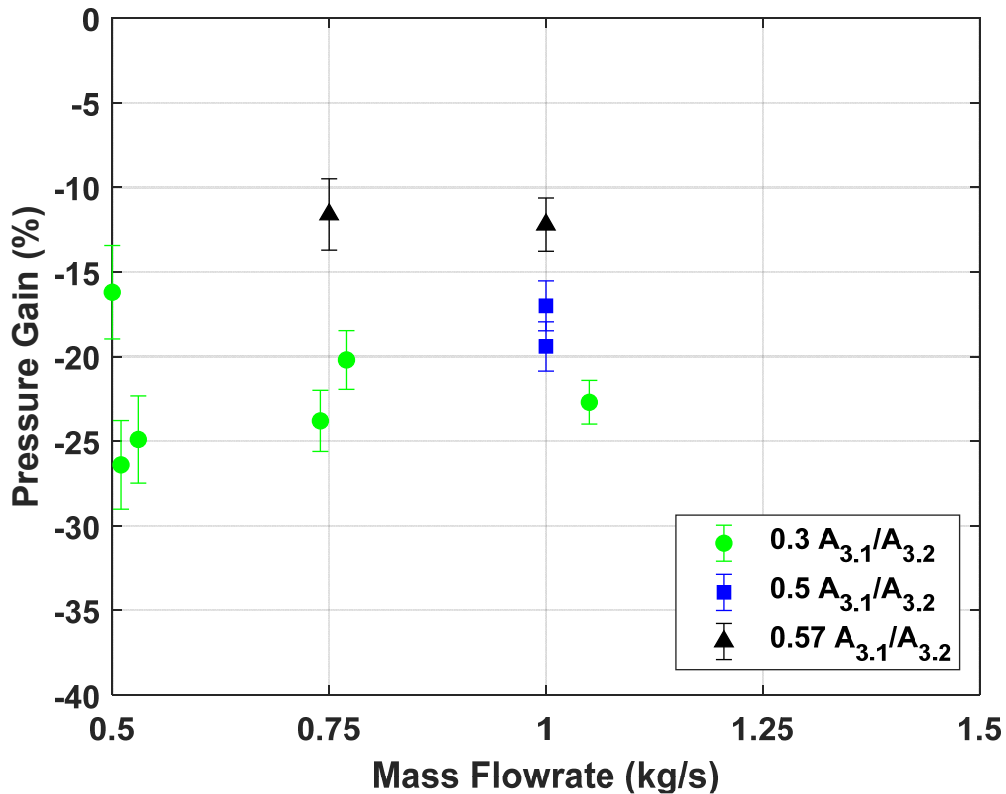
Figure 36.   Constant Equivalence Ratio for 0.68 $A_8/A_{3.2}$

Comparing the thrust of the combustor to the base drag, very few correlations can be determined. In Figure 37, there is no correlation between the base drag/ thrust and the exit area ratio. The 0.83 $A_8/A_{3.2}$ was tested at higher mass flowrates due to operability and therefore tended to have the higher thrust runs. Similarly, in Figure 38, there is no direct correlation between the base drag/ thrust and the air inlet value. The only visible correlation between the base drag and thrust is as thrust is increased the base drag also increases.
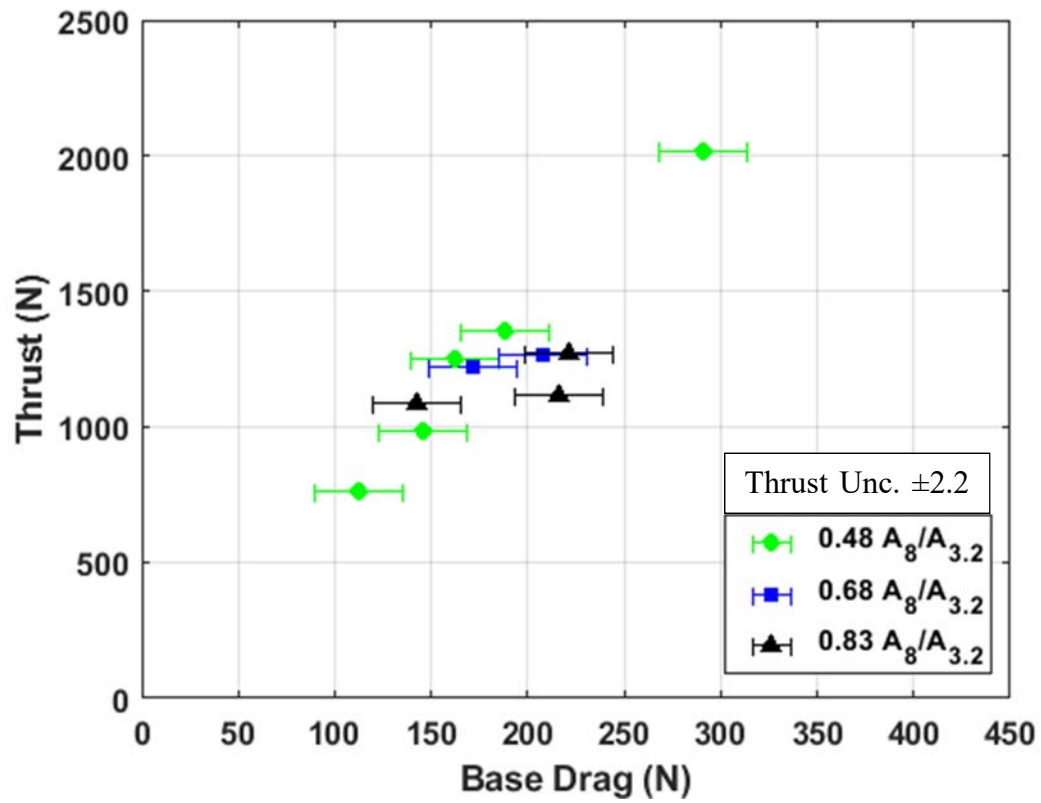
Figure 37.   Thrust versus Base Drag for a Constant 0.5 $A_{3.1}/A_{3.2}$
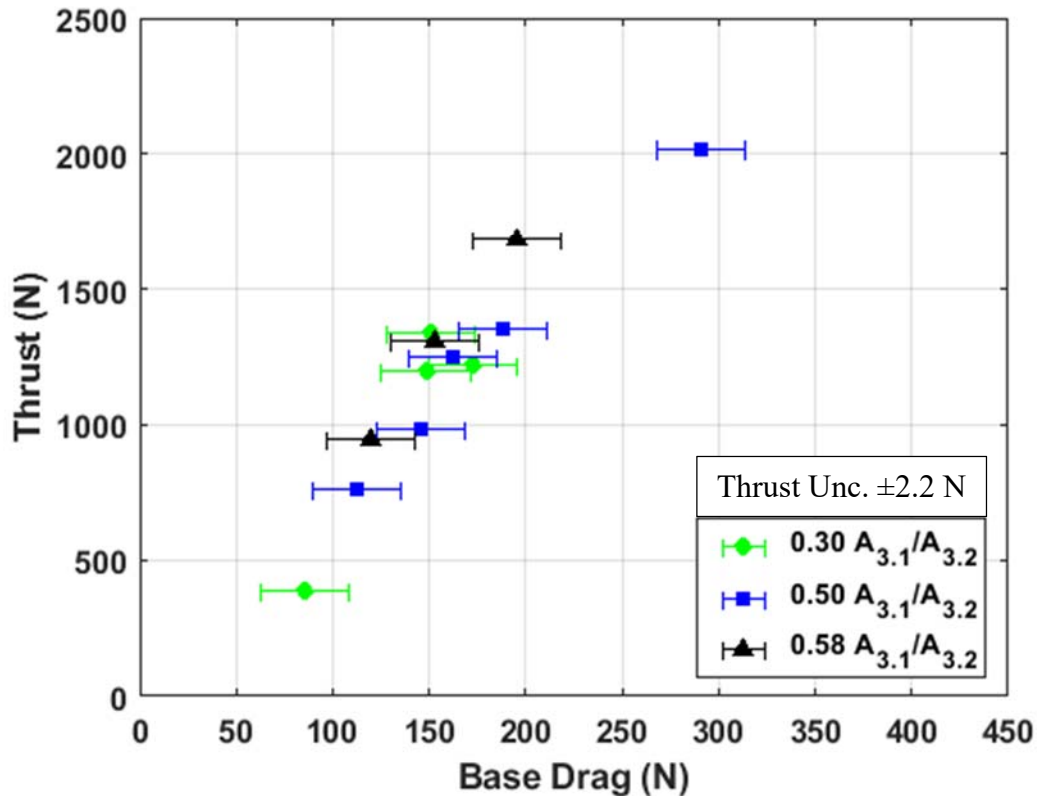
Figure 38.   Thrust versus Base Drag for 0.48 $A_8/A_{3.2}$

Validation is a vital aspect of the scientific process; EAP has never been experimentally calculated for an RDE, therefore the only method of validation is to compare to a computation model. The Kaemming and Paxson plot comparing $A_8/A_{3.2}$ and $A_{3.1}/A_{3.2}$ to a percent pressure gain, as depicted in Figure 23, was re-created with the experimental data overlaid in orange, shown in Figure 39. For both the computational and experimental values, a mass flowrate of 1.0 kg/s with an equivalence ratio of 1.0 was used. Kaemming and Paxson used three different air inlet ratios, 0.2, 0.4, and 0.6, whereas the experimental data used values of 0.3, 0.5, and 0.57 based off effective area measurements of the hardware. In the model, an ideal injector with perfect mixing of the oxidizer and fuel was implemented; however, the experimental injector is not an ideal system. Achieving defendable pressure gain performance would be momentous for the RDE community, but with the injector currently installed on the NPS rig, it is unlikely that global pressure gain will be demonstrated across the combustor. The jet in cross flow injector used has poor

mixing which leads to incomplete combustion. The poorly mixed reactants can lead to parasitic deflagration (pressure loss), or unreacted pockets of fuel and oxidizer (waste and spillage).; both scenarios lead to additional pressure loss in the combustor. The additional effect of heat loss, estimated at 10%, for the short duration tests also negatively affect the results.
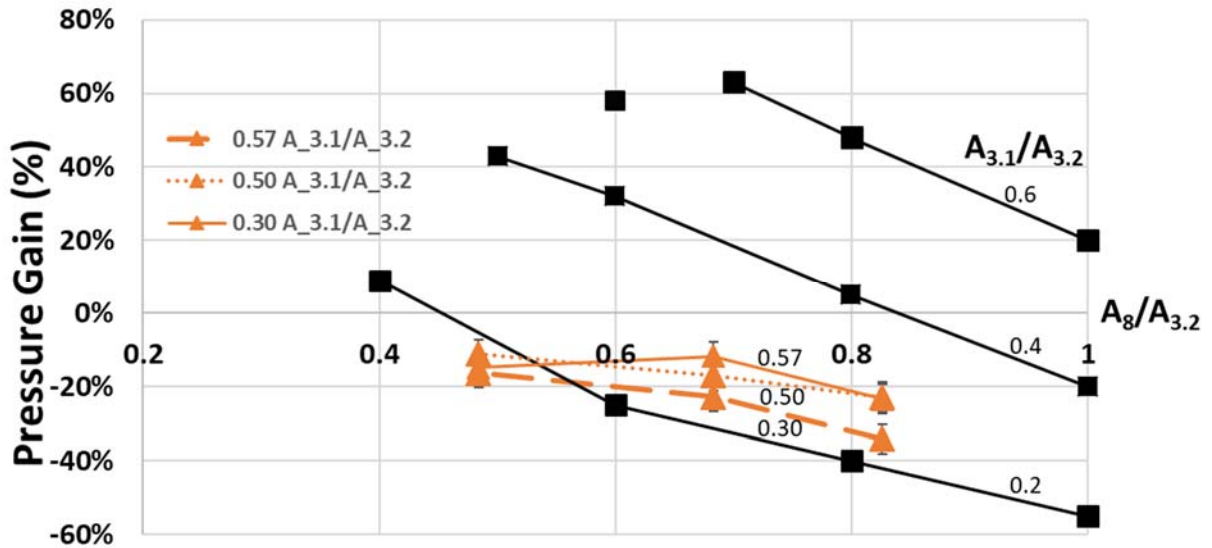
Figure 39.   Experimental Results Compared to Computational.
Adapted from Source: [6].

Due to experimental factors of added pressure losses, the pressure gain values seen experimentally, Figure 39, followed a similar trend to that of Figure 23 but not at the same magnitude of pressure gain. As exit area ratio decreases pressure gain increases, and as air inlet area increase pressure gain increases. The only point that fails to follow the convergence lines is the smallest exit restriction area with the largest air inlet gap. For this case, the air inlet area was larger than the exit area. Therefore, fluid would flow upstream if no momentum was pushing the fluid flowing towards the throat. Figure 23 displays one flagged point where the exit area was equal to the inlet area. The model was unable to converge as there was an oscillation in the mass flow rates [6]. A similar oscillation was seen in the experimental results; the detonation wave switched between an axial pulsing

and one wave detonation for the most restrictive exit area and most open inlet area. Therefore, the models appear to correlate well with the experimental results; although smaller $A_8/A_{3.2}$ and larger $A_{3.1}/A_{3.2}$ values produce better pressure gain, operability of the RDE starts to become an issue. If a more efficient injector was input into the same RDE setup, a larger pressure gain value could be achieved.

E.   CTAP CHAMBER ANALYSIS

The direct measurement and calculation of the EAP requires a very specific RDE set up to be computed. The engine must have a direct method of calculating thrust, a bluff body exit condition and a method of measure either the pressure or base drag force acting on the bluff body. Smaller research facilities may not have the capabilities to effectively determine the EAP for their engines; therefore, a CTAP line was placed near the exit of the channel just before the nozzle, as depicted in Figure 40. Due to hardware constraints the CTAP port was located 2.54 cm (1.0in) upstream of the throat.
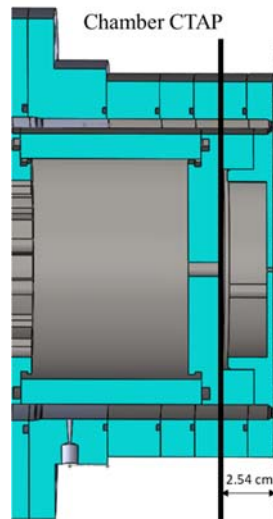
Figure 40.   Cross Sectional View of Chamber Pressure CTAP Location

The CTAP was placed flush with the chamber wall; as fluid flows by the port, the static pressure was recorded but not the dynamic pressure. EAP determines the total pressure of the chamber therefore the dynamic pressure must be accounted for in the CTAP

calculation of a chamber total pressure. Isentropic flow relations were used to convert the CTAP static pressure to a total pressure, as displayed in Equation 13.

$$\frac{p}{p_t} = \left(1 + \frac{\gamma - 1}{2} M^2\right)^{-\frac{\gamma}{\gamma-1}} \tag{13}$$

Since the Mach number in the chamber is theoretically determined by the $A_8/A_{3.2}$ when assuming steady flow, three different correction factors must be used for different geometries. Figure 41 displays the EAP calculations to the corrected CTAP measurements. CTAP pressure was written as "P_{T6} Experimental" to follow the common naming convention where the number follows the station and the 'T' represents a total stagnation pressure. The black line represents the ideal solution where EAP and the CTAP value display the same pressure if there is no pressure loss between the two stations. Error bars are not displayed for the data; however, it would display ±3.5, ±4.3, or ±6.0 kPa for the varying exit conditions for the EAP, and ± 5.7 kPa for the P_{T6} Experimental.
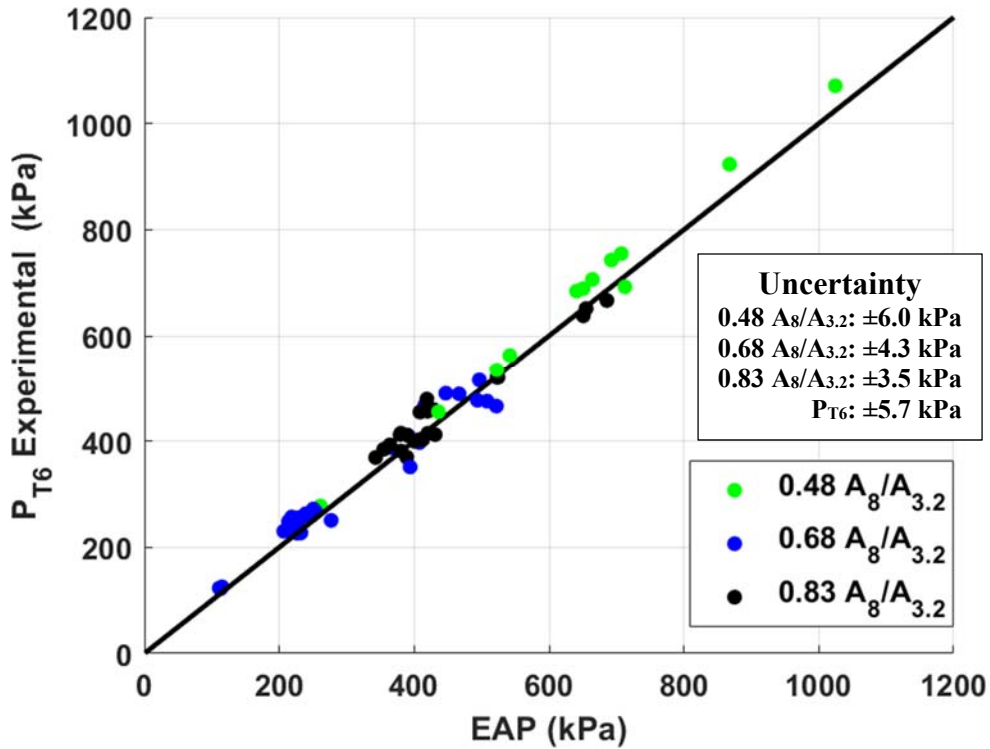
Figure 41.   Corrected CTAP Chamber Pressure Correlation to EAP

The two pressures follow the ideal trend line with minimal error for all detonation data. Therefore, from the supporting data, it appears that a corrected CTAP pressure can be used to measure the chamber pressure and be used for pressure gain measurements. More testing must be conducted utilizing different engine designs to validated this claim. If future data supports the claim, EAP will not be needed to calculate pressure gain. This will enable more engines and research centers to investigate the capabilities of an RDE. Figure 30 also shows that varying exit area ratio has little effect on the variation between the experimental and computed values.

F.   BRAYTON CYCLE COMPARISON

Although the experimental results showed global pressure loss in the RDE, the goal of RDEs is to display improved efficiency over a Brayton Cycle engine. In order to display the increased efficiency of an RDE, the global pressure loss of the RDE was compared to a theoretical Brayton Cycle ramjet engine. Chemical Equilibrium with Applications (CEA) is a NASA-designed code to determine thermodynamic states, and engine performance for complex mixture ratios. To create a direct comparison between the modeled ramjet and the experimental RDE, the 10th test case on April 17, 2019 was used. This run had a 0.78 kg/s air mass flow rate, equivalence ratio of 1.0, air inlet area ratio, $A_{3.1}/A_{3.2}$, of 0.50, exit area ratio of 0.48, $A_8/A_{3.2}$, and total pressure loss of 12.4% from the supply manifold to the combustor exit. The inlet to the injector for the RDE had a pressure of 618.7 kPa (89.7 psi) and an EAP of 543.9 kPa (78.9 psi). In CEA, several assumptions were made to create a modeled ramjet engine with similar parameters as the experimental RDE. The oxidizer to fuel ratio, the inverse of the equivalence ratio, was set at 1.0 or stochiometric. A finite area calculation was utilized with a chamber to throat area ratio ($A_{3.2}/A_8$) of 2.065 which is consistent with a chamber Mach number of 0.3.

Because CEA produces an idealized theoretical result, additional pressure loss terms were added to create a more realistic comparison. CEA takes into account Rayleigh losses across the combustor but does not include heat transfer, or flame holding effects. In a ramjet, flame holders are utilized to stabilize the flame used for combustion. Without the flame holders, the flame would be blown out of the engine before combustion could occur.

57

Flame holders are typically bluff bodies that restrict the flow and creates a lower speed recirculation region where the flame can remain continuous. By adding a restriction to the flow, however, pressure losses are induced. For a typical "V" shaped flame holder, Equation 12 can be used to characterize the pressure loss as per reference [22].

$$\%P_{loss} = 1.62\frac{\gamma}{2}M^2 \tag{12}$$

where γ is assumed to be 1.4 for air and the flow Mach number, M, is assumed to be 0.3. Utilizing Equation 12, the pressure loss percent due to flame holding was approximately 10% the initial pressure. A heat loss term must also be accounted for in this calculation. The RDE test runs only last a few seconds, therefore because there is a large temperature difference between the cold combustor walls and extremely hot combustion gases, an adiabatic system is highly unrealistic. This pressure loss was assumed to be between 10–20% but currently has not been determined for an RDE. Therefore, CEA was run assuming a 0–20% pressure losses due to heat transfer. CEA outputs a static pressure value at the injector, combustor end, and throat. Utilizing isentropic relations and Mach numbers of 0.0M, 0.297M, and 1.0M respectively the stagnation pressure at each location was evaluated. Pressure loss values from the injector to the throat are evaluated for the different theoretical models of the ramjet and are displayed in Table 7.

Table 7.   CEA Modeled Ramjet with Theoretical Losses

FLAME HOLDING LOSS (%)	HEAT TRANSFER LOSS (%)	INITIAL INJECTOR (kPa)	INJECTOR + LOSSES (kPa)	COMBUSTOR END (kPa)	THROAT (kPa)	PRESSURE GAIN (%)
0	0	618.7	618.7	587.1	585.5	-5.4
10	0	618.7	556.8	528.5	526.6	-14.9
10	5	618.7	529.0	502.8	500.4	-19.1
10	10	618.7	501.2	475.3	474.1	-23.4
10	15	618.7	473.3	448.9	447.8	-27.6
10	20	618.7	445.5	422.5	421.5	-31.9

The RDE with the same specifications as the theoretically experimental ramjet produced a pressure gain of -12.4%. Therefore, just by assuming there is a pressure loss from flame holding and the combustor is adiabatic, the RDE already outperforms the Brayton Cycle engine. When compared to more realistic heat transfer losses, 10–15 %, the RDE has less than half the pressure loss across the combustor. By having a decreased pressure loss with all other parameters remaining constant, the overall efficiency of the combustor increased; therefore, at this configuration the RDE would be able to outperform a ramjet engine under similar inlet and operating conditions.

THIS PAGE INTENTIONALLY LEFT BLANK

V. CONCLUSIONS

A. SUMMARY OF RESULTS

The objective of this work was to experimentally calculate EAP, investigate how geometry changes effect EAP and pressure gain, compare experimental EAP results to nondimensionalized computational results, and compare experimental EAP values of an RDE to CEA chamber pressures of an analogous Brayton Cycle ramjet engine. EAP was calculated utilizing base drag, thrust, and ambient pressure measurements. The air inlet area and throat exit area were modified while keeping chamber area constant to produce nine different geometry configurations. As air inlet area increased, the flow is able to travel through the restriction easier, therefore the pressure loss across the restriction decreases. By decreasing this pressure loss term, the pressure gain across the combustor increases. Chamber Mach number is directly related to the exit area, A_8, compared to the chamber area, $A_{3.2}$, As exit area increases, the chamber Mach number also approached a sonic condition. By increasing the velocity of the flow, the static pressure within the chamber decreases and the refresh rate increases. Because the initial static pressure is lower, the detonation jump condition produces a lower final static pressure. The lower static pressure leads to lower total pressure and lower pressure gain across the combustor. Therefore, by increasing exit area ratio, $A_8/A_{3.2}$, the pressure gain of the combustor decreases. The experimental EAP results follow the theoretical trends.

The experimental results were compared to computational results provided by Kaemming and Paxson [6]. The nondimensionalized ratios of air inlet area and exit area compared to chamber area enabled their results to be compared to any air breathing hydrogen fueled RDE operating on similar conditions, mass flowrate of air at 1.0 kg/s and at stochiometric. The experimental results followed the same trends as the modeling; however, the magnitude of the pressure gain percentage was noticeably lower for the experimental values due to injector losses, decreased combustion efficiency, and heat losses. Though a pressure gain result was not achieved, the purpose of this work was to display the capability of determining the pressure gain across an RDE. The combination of

non-ideal conditions such as heat loss, combustion efficiency, and other pressure loss processes within the experimental combustor resulted net pressure losses.

The EAP calculations were compared to a direct CTAP static chamber pressure measurement at the combustor exit. Both calculations started with a static pressure measurement then isentropic relations were used to translate to total pressure. For EAP, calculated at the throat, the Mach number was assumed to be 1.0. For the CTAP measurements, the Mach number was dependent on which exit area restriction was being utilized for the test. The resulting total pressures produced almost identical results. More research must be conducted for different geometry RDE set ups to determine if a simple corrected CTAP static chamber pressure measurement produces a valid time averaged chamber pressure. If this approach is validated by other data, research facilities without the capabilities to measure the base drag and thrust of the RDE could still calculate the pressure gain performance of their device.

Finally, the RDE's pressure gain was compared to a theoretical ramjet engine operating under similar conditions. The same injector pressure, area restriction, and fuel mixture type and ratio was utilized to design an idealized ramjet with only Rayleigh losses; then additional total pressure losses of flame holding and heat transfer were added to create a theoretical experimental ramjet. With an assumed 10% loss of both flame holding and heat transfer, the RDE was shown to deliver half the pressure loss across the combustor. This comparison displays the capabilities and possible implications of implementing RDEs. By decreasing pressure losses, the total efficiency of the engine increases.

B.   FUTURE WORK

Though this thesis helped verify the experimental calculation of pressure gain/loss in an RDE, it leaves several areas for future work. EAP is calculated to show the pressure gain across a combustor; the engine geometry and injector displayed in this thesis was not capable of achieving pressure gain, but did show improvement over a conventional ramjet engine. Future research requires an injector with better combustion efficiency or a different geometry to achieve pressure gain. Additionally, computational modeling of the test RDE

with accurate combustion efficiency should be used to provide additional validation to the experimental results.

The EAP calculation requires a very specific engine set up with a base drag bluff body capable or measuring the drag force acting upon it. The rig in TC2 of the NPS RPCL provided the perfect set up for this specific measurement as the center body of the rig was hollow for data lines to run through. Other research centers do not have the same engine design but still desire to show the efficiency of their combustors. The static pressure CTAP line in the chamber shows promise in being an effective way to measure the EAP of an RDE. This would require minimal hardware to be implemented and could be used on almost any engine design. Future research into other geometries, injectors, and engine designs is necessary before this measurement can be used for pressure gain measurements. By proving a simple static pressure measurement, converted to total pressure with isentropic relations, combustors all over the world could easily compare RDE combustor efficiency. Experimental EAP calculations are just one small step towards displaying the full capabilities and uses of an RDE.

THIS PAGE INTENTIONALLY LEFT BLANK

APPENDIX A. EXPERIMENTAL RUNS

Below is the table of all experimental runs used for this thesis. This test campaign started March 13, 2019, and ended April 19, 2019. All tests were conducted in TC2 at the NPS RPCL.

Date	Run Number	$\dot{m}_{air}$ (kg/s)	Equivalence Ratio	Exit Area ($A_8/A_{3.2}$)	Thrust (N)	Chamber CTAP (kPa)	Base Drag (N)	Air Plenum (kPa)	EAP (kPa)	Press Gain (%)
				0.30 $A_{3.1}/A_{3.2}$						
18-Mar-19	2	0.44	0.70	0.48	299	263	-86	321	261	-18.7
18-Mar-19	8	1.01	0.84	0.48	1050	647	-148	770	641	-16.8
18-Mar-19	9	1.01	0.87	0.48	1047	652	-173	778	651	-16.3
18-Mar-19	10	1.01	1.13	0.48	1189	714	-151	852	707	-17.0
14-Mar-19	7	0.50	0.60	0.68	115	111	15	186	115	-38.0
14-Mar-19	6	0.47	0.64	0.68	91	108	-4	175	113	-35.2
14-Mar-19	5	0.45	0.67	0.68	104	109	16	170	111	-34.8
14-Mar-19	8	0.50	0.71	0.68	346	203	-25	289	207	-28.4
14-Mar-19	9	0.51	0.77	0.68	374	216	-21	305	215	-29.7
14-Mar-19	1	0.52	0.86	0.68	385	227	-21	319	219	-31.5
14-Mar-19	3	0.50	0.89	0.68	375	220	-17	308	214	-30.6
14-Mar-19	13	0.53	0.91	0.68	421	229	-47	329	240	-27.1
14-Mar-19	10	0.51	0.93	0.68	412	226	-26	322	229	-28.7
14-Mar-19	14	0.53	0.94	0.68	429	240	-71	333	250	-24.8
13-Mar-19	3	0.51	0.96	0.68	405	232	-61	324	239	-26.3
22-Mar-19	3	0.50	0.99	0.68	401	221	-177	329	277	-15.8
16-Apr-19	5	0.47	1.04	0.68	354	201	-91	311	232	-25.4
16-Apr-19	4	0.47	1.04	0.68	352	200	-77	313	226	-27.7
14-Mar-19	15	0.47	1.05	0.68	387	220	-45	307	228	-25.9
14-Mar-19	11	0.50	1.17	0.68	429	235	-83	332	254	-23.3
15-Mar-19	2	0.74	1.01	0.68	707	342	-134	479	366	-23.6
22-Mar-19	2	0.77	0.99	0.68	778	351	-188	510	408	-20.0
15-Mar-19	1	0.81	0.93	0.68	766	362	-151	514	392	-23.8
15-Mar-19	4	1.04	0.60	0.68	896	413	-93	578	416	-28.1

15-Mar-19	6	1.02	0.71	0.68	918	433	-163	604	447	-26.1
15-Mar-19	7	1.02	0.80	0.68	995	432	-144	621	467	-24.9
15-Mar-19	8	1.06	0.85	0.68	1079	455	-149	653	497	-24.0
18-Mar-19	1	1.05	1.00	0.68	1120	460	-186	675	523	-22.6
5-Apr-19	4	1.03	0.60	0.83	797	301	-154	537	343	-36.2
5-Apr-19	3	1.02	0.68	0.83	841	313	-153	551	355	-35.5
5-Apr-19	1	1.01	0.74	0.83	865	320	-163	562	364	-35.2
3-Apr-19	2	1.03	0.81	0.83	935	336	-147	589	379	-35.7
3-Apr-19	1	1.02	0.83	0.83	935	338	-151	588	380	-35.4
8-Apr-19	3	1.00	0.86	0.83	1032	371	-157	588	408	-30.5
2-Apr-19	1	1.00	0.88	0.83	939	335	-182	589	390	-33.9
2-Apr-19	2	1.01	0.92	0.83	975	329	-215	596	409	-31.4
11-Apr-19	1	1.01	0.96	0.83	1096	372	-135	556	420	-24.5
10-Apr-19	6	1.02	0.96	0.83	1117	374	-124	518	423	-18.5
16-Apr-19	10	0.97	1.00	0.83	967	328	-236	590	412	-30.1
8-Apr-19	2	1.00	1.02	0.83	1124	391	-103	620	419	-32.4
8-Apr-19	1	0.99	1.04	0.83	1104	374	-161	607	429	-29.2
16-Apr-19	3	1.22	1.07	0.83	1327	424	-283	752	524	-30.3
16-Apr-19	2	1.53	1.02	0.83	1692	531	-393	929	655	-29.5
16-Apr-19	1	1.55	1.15	0.83	1760	543	-436	972	686	-29.4
				0.50 $A_{3.1}/A_{3.2}$						
17-Apr-19	11	0.47	1.06	0.48	125	145	-13	173	146	-15.6
17-Apr-19	12	0.64	1.00	0.48	647	431	-113	501	436	-12.9
17-Apr-19	10	0.78	1.00	0.48	841	532	-146	619	542	-12.4
18-Apr-19	2	0.96	1.06	0.48	1087	668	-162	772	664	-13.9
17-Apr-19	9	1.00	1.03	0.48	1164	655	-188	775	712	-8.1
18-Apr-19	1	1.49	0.98	0.48	1730	1013	-291	1174	1024	-12.7
17-Apr-19	6	1.02	0.93	0.68	1012	407	-337	605	538	-11.1

17-Apr-19	7	1.00	1.04	0.68	1054	420	-208	611	508	-16.8
17-Apr-19	8	1.00	1.04	0.68	1048	421	-172	612	494	-19.3
17-Apr-19	4	0.98	0.79	0.83	294	138	-22	241	168	-30.0
17-Apr-19	5	0.98	0.82	0.83	902	301	-216	511	389	-24.0
17-Apr-19	2	0.99	0.94	0.83	946	311	-143	530	381	-28.2
17-Apr-19	3	1.03	0.98	0.83	1049	336	-222	563	431	-23.4
				0.58 $A_{3.1}/A_{3.2}$						
19-Apr-19	12	0.78	0.99	0.48	826	506	-119	593	523	-11.9
19-Apr-19	11	1.03	1.00	0.48	1156	703	-153	812	692	-14.8
19-Apr-19	10	1.28	1.03	0.48	1489	873	-195	1012	868	-14.3
19-Apr-19	8	0.75	0.96	0.68	681	310	-244	443	394	-11.1
19-Apr-19	6	1.00	0.98	0.68	1011	412	-292	592	522	-11.8
19-Apr-19	9	1.26	0.91	0.68	1413	838	-193	969	624	-35.6
19-Apr-19	7	1.27	0.96	0.68	1405	523	-279	754	651	-13.7
19-Apr-19	1	1.00	1.08	0.83	994	326	-166	537	401	-25.4
19-Apr-19	3	1.03	0.97	0.83	1025	338	-207	548	420	-23.3
19-Apr-19	4	1.52	0.95	0.83	1667	520	-402	828	651	-21.4

APPENDIX B. MATLAB CODE

```matlab
clear all
close all
clc

[fname, floc, dum] = uigetfile;
load(strcat(floc,fname));

A={sprintf('Start Time for Calculating Averages'),...
    sprintf('End Time for Calculating Averages'),...
    sprintf('Row in Excel Doc'),...
    sprintf('before Mar 22 (yes or no)')};
title='User_inputs';
lines=1;
defaultval={num2str(3.5),num2str(3.5),num2str(1),'no'};
answer=inputdlg(A,title,lines,defaultval);
drawnow; pause(0.05);

startval=(str2num(answer{1})*2000);
endval=(str2num(answer{2})*2000);
Time=1:20600;
Time=Time/2000;
h2sup=d.data1(:,3);
airsup=d.data1(:,7);
h2plen=d.data1(:,9);
if answer{4}=='no'
    airplen=d.data1(:,12);
else
airplenold=d.data1(:,12);
airplenV=(airplenold+125)/125;
airplen=airplenV*49.53131-49.1331;


end

thrust=d.data1(:,21);
mdotair=d.data1(:,22);
mdoth2=d.data1(:,23);
phi=d.data1(:,25);
mdotair0=mdotair;
phi0=phi;
airplen_SI=(14.7+airplen)*6.89476;
thrust_SI=4.44822*thrust;

h2supstd=std(h2sup(startval:endval));
h2sup=mean(h2sup(startval:endval));
airsupstd=std(airsup(startval:endval));
airsup=mean(airsup(startval:endval));
h2plenstd=std(h2plen(startval:endval));
h2plen=mean(h2plen(startval:endval));
airplenstd=std(airplen(startval:endval));
```

69

```matlab
airplen=mean(airplen(startval:endval));
thruststd=std(thrust(startval:endval));
thrust=mean(thrust(startval:endval));
mdotairstd=std(mdotair(startval:endval));
mdotair=mean(mdotair(startval:endval));
mdoth2std=std(mdoth2(startval:endval));
mdoth2=mean(mdoth2(startval:endval));
phistd=std(phi(startval:endval));
phi=mean(phi(startval:endval));
airplen_abs=airplen+14.7;
x=[mdotair,phi,thrust,airplen,airplen_abs,h2sup,airsup,mdoth2];
y=[mdotairstd,phistd,thruststd,airplenstd,h2plenstd,airsupstd,mdoth2std
];
row=(str2num(answer{3}));
LocA=strcat('C',answer{3});
LocB=strcat('BB',answer{3});
xlswrite('testdata2.xlsx',x,1,LocA)
xlswrite('testdata2.xlsx',y,1,LocB)

figure;
yyaxis left
plot(Time,thrust_SI);
xlabel('Time (sec)')
ylabel('Thrust (N)')
yyaxis right
plot(Time,phi0)
ylabel('Equivalence Ratio')

figure;
yyaxis left
plot(Time,mdotair0);
xlabel('Time (sec)')
ylabel('Air Massflow Rate (kg/s)')
yyaxis right
plot(Time,airplen_SI)
ylabel('Air Plenum Pressure (kPa)')


clear all
close all
clc

%% Pick the Excel File

% Ideally bring in two documents, one with Thrust one with Mobile DAC
data

[fname floc dum] = uigetfile;

volt = xlsread(strcat(floc,fname));

% volt=xlsread(DATAFILE);

%% Runs March 13-March 15 Run 02
```

```matlab
%  Pick Pressurechoice=1
%% Runs March 15 Run 03- March 19
%  Pick Pressurechoice=2
%% Runs March 22-March Run03
%  Pick Pressurechoice=3
%% Runs March22 Run04-Present
%  Pick Pressurechoice=4




pressurechoice=4;




%% Pressures

[Press] = getPres(volt,pressurechoice);                      %Creates
Pressure in PSIG
T=0.001:0.001:10;
%% Average Pressure
Press_SI=(Press+14.7)*6.894757;
figure;
plot(T,Press_SI)
title(strrep(fname,'.xlsx',''));
xlabel('Time (sec)')
ylabel('Pressure (kPa)')
grid on
ylim([80 110]);
xlim([0 6]);

figure;
plot(T,volt)
title(strrep(fname,'.xlsx',''));
xlabel('time(sec)')
ylabel('Voltage (V)')
grid on

saveas(gcf,strrep(fname,'.xlsx','.fig'));
saveas(gcf,strrep(fname,'.xlsx','.jpg'));
A={sprintf('Start Time for Calculating Averages'),...
    sprintf('End Time for Calculating Averages'),...
    sprintf('Row in Excel Doc')};
xtitle='User_inputs';
lines=1;
defaultval={num2str(1.5),num2str(2.0),num2str(1)};
answer=inputdlg(A,xtitle,lines,defaultval);
drawnow; pause(0.05);

startval=(str2num(answer{1})*1000);
endval=(str2num(answer{2})*1000);
```

71

```matlab
[Pavg,Pavgstd] = Pressavg(Press,startval,endval);
%Pressure in PSIG

%% Pressure Converison

Pavg_SI=(Pavg)*6894.757;                              %Converts to Pa


row=(str2num(answer{3}));
LocA=strcat('R',answer{3});
LocB=strcat('BJ',answer{3});
% xlswrite('testdata2.xlsx',Pavg,1,LocA)
% xlswrite('testdata2.xlsx',Pavgstd,1,LocB)


function [Press] = getPres(aiall,pressurechoice)
% ai0=smooth(smooth(aiall(:,1)));
% ai1=smooth(smooth(aiall(:,2)));
% ai2=smooth(smooth(aiall(:,3)));
% ai3=smooth(smooth(aiall(:,4)));
% ai4=smooth(smooth(aiall(:,5)));
% ai5=smooth(smooth(aiall(:,6)));
% ai6=smooth(smooth(aiall(:,7)));
% ai7=smooth(smooth(aiall(:,8)));
% ai8=smooth(smooth(aiall(:,9)));
% ai9=smooth(smooth(aiall(:,10)));
% ai10=smooth(smooth(aiall(:,11)));
% ai11=smooth(smooth(aiall(:,12)));
% ai12=smooth(smooth(aiall(:,13)));
% ai13=smooth(smooth(aiall(:,14)));
ai0=aiall(:,1);
ai1=aiall(:,2);
ai2=aiall(:,3);
ai3=aiall(:,4);
ai4=aiall(:,5);
ai5=aiall(:,6);
ai6=aiall(:,7);
ai7=aiall(:,8);
ai8=aiall(:,9);
ai9=aiall(:,10);
ai10=aiall(:,11);
ai11=aiall(:,12);
ai12=aiall(:,13);
ai13=aiall(:,14);

if pressurechoice==1;
    ai0slope=-2.94;
    ai0int=2.94;
    ai1slope=-2.94;
    ai1int=2.94;
    ai2slope=-2.94;
    ai2int=2.94;
    ai3slope=7.5;
    ai3int=-22.2;
```

```
        ai4slope=7.5;
        ai4int=-22.2;
        ai5slope=-3.675;
        ai5int=3.675;
        ai6slope=-3.675;
        ai6int=3.675;
        ai7slope=-3.675;
        ai7int=3.675;
        ai8slope=-3.675;
        ai8int=3.675;
        ai9slope=-3.675;
        ai9int=3.675;
        ai10slope=-3.675;
        ai10int=3.675;
        ai11slope=-3.675;
        ai11int=3.675;
        ai12slope=49.78815;
        ai12int=-51.1195;
        ai13slope=49.72488;
        ai13int=-50.6166;

elseif pressurechoice==2;

        ai0slope=-2.94;
        ai0int=2.94;
        ai1slope=-2.94;
        ai1int=2.94;
        ai2slope=-2.94;
        ai2int=2.94;
        ai10slope=7.5;
        ai10int=-22.2;
        ai11slope=7.5;
        ai11int=-22.2;
        ai5slope=-3.675;
        ai5int=3.675;
        ai6slope=-3.675;
        ai6int=3.675;
        ai7slope=-3.675;
        ai7int=3.675;
        ai8slope=-3.675;
        ai8int=3.675;
        ai9slope=-3.675;
        ai9int=3.675;
        ai3slope=-3.675;
        ai3int=3.675;
        ai4slope=-3.675;
        ai4int=3.675;
        ai12slope=49.78815;
        ai12int=-51.1195;
        ai13slope=49.72488;
        ai13int=-50.6166;

elseif pressurechoice==3;
```

```matlab
    ai0slope=49.53131;          %200psig transducer 61117533 changed on
03/22/19
    ai0int=-49.1331;
    ai1slope=7.5;               %15&VAC transducer changed 03/22/19
    ai1int=-22.2;
    ai2slope=7.5;               %15&VAC transducer changed 03/22/19
    ai2int=-22.2;
    ai3slope=-3.675;
    ai3int=3.675;
    ai4slope=-3.675;
    ai4int=3.674;
    ai5slope=-3.675;
    ai5int=3.675;
    ai6slope=-3.675;
    ai6int=3.675;
    ai7slope=-3.675;
    ai7int=3.675;
    ai8slope=-3.675;
    ai8int=3.675;
    ai9slope=-3.675;
    ai9int=3.675;
    ai10slope=7.5;
    ai10int=-22.2;
    ai11slope=7.5;
    ai11int=-22.2;
    ai12slope=49.78815;
    ai12int=-51.1195;
    ai13slope=49.72488;
    ai13int=-50.6166;

else

    ai0slope=49.53131;          %200psig transducer 61117533 changed on
03/22/19
    ai0int=-49.1331;
    ai9slope=7.5;               %15&VAC transducer changed 03/22/19
    ai9int=-22.2;
    ai8slope=7.5;               %15&VAC transducer changed 03/22/19
    ai8int=-22.2;
    ai3slope=-3.675;
    ai3int=3.675;
    ai4slope=-3.675;
    ai4int=3.674;
    ai5slope=-3.675;
    ai5int=3.675;
    ai6slope=-3.675;
    ai6int=3.675;
    ai7slope=-3.675;
    ai7int=3.675;
    ai1slope=-3.675;
    ai1int=3.675;
    ai2slope=-3.675;
    ai2int=3.675;
    ai10slope=7.5;
    ai10int=-22.2;
```

74

```matlab
    ai11slope=7.5;
    ai11int=-22.2;
    ai12slope=49.78815;
    ai12int=-51.1195;
    ai13slope=49.72488;
    ai13int=-50.6166;
end

Pai0=ai0slope*ai0+ai0int;
Pai1=ai1slope*ai1+ai1int;
Pai2=ai2slope*ai2+ai2int;
Pai3=ai3slope*ai3+ai3int;
Pai4=ai4slope*ai4+ai4int;
Pai5=ai5slope*ai5+ai5int;
Pai6=ai6slope*ai6+ai6int;
Pai7=ai7slope*ai7+ai7int;
Pai8=ai8slope*ai8+ai8int;
Pai9=ai9slope*ai9+ai9int;
Pai10=ai10slope*ai10+ai10int;
Pai11=ai11slope*ai11+ai11int;
Pai12=ai12slope*ai12+ai12int;
Pai13=ai13slope*ai13+ai13int;

Press=[Pai0,Pai1,Pai2,Pai3,Pai4,Pai5,Pai6,Pai7,Pai8,Pai9,Pai10,Pai11,Pa
i12,Pai13];

end

clear all
close all
clc

Airplen=xlsread('Testdata2.xlsx','F72:F72');
Airplen_abs=Airplen+14.7;
F_th=xlsread('Testdata2.xlsx','E72:E72');
%Pavg=xlsread('Testdata2.xlsx','R75:AE75');
Pavg=xlsread('Testdata2.xlsx','AH72:AU72');
% Pressure Converison

Pavg_SI=Pavg*6894.757;                          %Converts to Pa

%% Calculate Base Drag

Base_Drag_Net = BaseDrag(Pavg_SI);              %Produced Base Drag in N
Base_Drag_lbf=Base_Drag_Net/4.448;
%% Calculate EAP

F_th_SI=F_th*4.44822;          %N
P_amb=101352.9;                %Pa
A_exit=xlsread('Testdata2.xlsx','O72:O72');          %in^2
A_exit_SI=A_exit/1550.003;  %m^2
Gamma=1.24;
M_exit=1;
```

75

```matlab
T8_SI=((F_th_SI+P_amb.*A_exit_SI-
Base_Drag_Net)./((1+Gamma*(M_exit^2)).*A_exit_SI));
EAP_SI=T8_SI*(((Gamma+1)/2)^(Gamma/(Gamma-1)));
EAP_abs=EAP_SI/6894.757;
EAP_gauge=EAP_abs-14.7;
Pgain=((EAP_abs-Airplen_abs)./Airplen_abs)*100;


X=[Base_Drag_lbf,EAP_abs,EAP_gauge,Pgain];

function [Pavg,Pavgstd] = Pressavg(Press,startval,endval)
Pai0avg=mean(Press(startval:endval,1));
Pai0std=std(Press(startval:endval,1));
Pai1avg=mean(Press(startval:endval,2));
Pai1std=std(Press(startval:endval,2));
Pai2avg=mean(Press(startval:endval,3));
Pai2std=std(Press(startval:endval,3));
Pai3avg=mean(Press(startval:endval,4));
Pai3std=std(Press(startval:endval,4));
Pai4avg=mean(Press(startval:endval,5));
Pai4std=std(Press(startval:endval,5));
Pai5avg=mean(Press(startval:endval,6));
Pai5std=std(Press(startval:endval,6));
Pai6avg=mean(Press(startval:endval,7));
Pai6std=std(Press(startval:endval,7));
Pai7avg=mean(Press(startval:endval,8));
Pai7std=std(Press(startval:endval,8));
Pai8avg=mean(Press(startval:endval,9));
Pai8std=std(Press(startval:endval,9));
Pai9avg=mean(Press(startval:endval,10));
Pai9std=std(Press(startval:endval,10));
Pai10avg=mean(Press(startval:endval,11));
Pai10std=std(Press(startval:endval,11));
Pai11avg=mean(Press(startval:endval,12));
Pai11std=std(Press(startval:endval,12));
Pai12avg=mean(Press(startval:endval,13));
Pai12std=std(Press(startval:endval,13));
Pai13avg=mean(Press(startval:endval,14));
Pai13std=std(Press(startval:endval,14));

Pavg=[Pai0avg,Pai1avg,Pai2avg,Pai3avg,Pai4avg,...
    Pai5avg,Pai6avg,Pai7avg,Pai8avg,Pai9avg,...
    Pai10avg,Pai11avg,Pai12avg,Pai13avg];
Pavgstd=[Pai0std,Pai1std,Pai2std,Pai3std,Pai4std,...
    Pai5std,Pai6std,Pai7std,Pai8std,Pai9std,...
    Pai10std,Pai11std,Pai12std,Pai13std];
end


clear all
close all
clc

%% Excel Read In
```

```matlab
phi=xlsread('ThesisData.xlsx','D4:D49');
mdot=xlsread('ThesisData.xlsx','C4:C49');
A=xlsread('ThesisData.xlsx','E4:E49');
pgain=xlsread('ThesisData.xlsx','K4:K49');
det=xlsread('ThesisData.xlsx','L4:L49');
Thrust=xlsread('ThesisData.xlsx','F4:F49');
EAP=xlsread('ThesisData.xlsx','J4:J49');
Drag=xlsread('ThesisData.xlsx','H4:H49');
CTAP=xlsread('ThesisData.xlsx','G4:G49');
Eavg=xlsread('ThesisData.xlsx','Y4:Y49');
Thrust=Thrust-Drag;


phi02=xlsread('ThesisData.xlsx','D51:D61');
mdot02=xlsread('ThesisData.xlsx','C51:C61');
A02=xlsread('ThesisData.xlsx','E51:E61');
pgain02=xlsread('ThesisData.xlsx','K51:K61');
det02=xlsread('ThesisData.xlsx','L51:L61');
Thrust02=xlsread('ThesisData.xlsx','F51:F61');
EAP02=xlsread('ThesisData.xlsx','J51:J61');
Drag02=xlsread('ThesisData.xlsx','H51:H61');
CTAP02=xlsread('ThesisData.xlsx','G51:G61');
Eavg02=xlsread('ThesisData.xlsx','Y51:Y61');
Thrust02=Thrust02-Drag02;


phi03=xlsread('ThesisData.xlsx','D63:D73');
mdot03=xlsread('ThesisData.xlsx','C63:C73');
A03=xlsread('ThesisData.xlsx','E63:E73');
pgain03=xlsread('ThesisData.xlsx','K63:K73');
det03=xlsread('ThesisData.xlsx','L63:L73');
Thrust03=xlsread('ThesisData.xlsx','F63:F73');
EAP03=xlsread('ThesisData.xlsx','J63:J73');
Drag03=xlsread('ThesisData.xlsx','H63:H73');
CTAP03=xlsread('ThesisData.xlsx','G63:G73');
Eavg03=xlsread('ThesisData.xlsx','Y63:Y73');
Thrust03=Thrust03-Drag03;
%% Numbering Initial Values
X=1;
Y=1;
Z=1;
Xno=1;
Yno=1;
Zno=1;
X02=1;
Y02=1;
Z02=1;
Xno02=1;
Yno02=1;
Zno02=1;
X03=1;
Y03=1;
Z03=1;
```

77

```matlab
Xno03=1;
Yno03=1;
Zno03=1;

%% Seperation of Data

for i=1:length(phi)
%     if mdot(i)<=1.06 && mdot(i)>=0.94

    if A(i)==0.48
            if det(i)==0
                color='r';
                phi03no(Xno)=phi(i);
                mdot03no(Xno)=mdot(i);
                pgain03no(Xno)=pgain(i);
                det03no(Xno)=det(i);
                A03no(Xno)=A(i);
                Thrustno(Xno)=Thrust(i);
                EAPno(Xno)=EAP(i);
                Dragno(Xno)=Drag(i);
                CTAPno(Xno)=CTAP(i);
                Eavgno(Xno)=Eavg(i);
                Xno=Xno+1;
            else
                phi030(X)=phi(i);
                mdot030(X)=mdot(i);
                pgain030(X)=pgain(i);
                det030(X)=det(i);
                A030(X)=A(i);
                Thrust030(X)=Thrust(i);
                EAP030(X)=EAP(i);
                Drag030(X)=Drag(i);
                CTAP030(X)=CTAP(i);
                Eavg030(X)=Eavg(i);
                X=X+1;
            end
    elseif A(i)==0.68
        color='b';
            if det(i)==0
                color='r';
                phi045no(Yno)=phi(i);
                mdot045no(Yno)=mdot(i);
                pgain045no(Yno)=pgain(i);
                det045no(Yno)=det(i);
                A045no(Yno)=A(i);
                Thrust045no(Yno)=Thrust(i);
                EAP045no(Yno)=EAP(i);
                Drag045no(Yno)=Drag(i);
                CTAP045no(Yno)=CTAP(i);
                Eavg045no(Yno)=Eavg(i);
                Yno=Yno+1;
            else
                phi045(Y)=phi(i);
                mdot045(Y)=mdot(i);
                pgain045(Y)=pgain(i);
```

78

```matlab
                    det045(Y)=det(i);
                    A045(Y)=A(i);
                    Thrust045(Y)=Thrust(i);
                    EAP045(Y)=EAP(i);
                    Drag045(Y)=Drag(i);
                    CTAP045(Y)=CTAP(i);
                    Eavg045(Y)=Eavg(i);
                    Y=Y+1;
                end
    elseif A(i)==0.83
            if det(i)==0
                color='r';
                phi058no(Zno)=phi(i);
                mdot058no(Zno)=mdot(i);
                pgain058no(Zno)=pgain(i);
                det058no(Zno)=det(i);
                A058no(Zno)=A(i);
                Thrust058no(Zno)=Thrust(i);
                EAP058no(Zno)=EAP(i);
                Drag058no(Zno)=Drag(i);
                CTAP058no(Zno)=CTAP(i);
                Eavg058no(Zno)=Eavg(i);
                Zno=Zno+1;
            else
                phi058(Z)=phi(i);
                mdot058(Z)=mdot(i);
                pgain058(Z)=pgain(i);
                det058(Z)=det(i);
                A058(Z)=A(i);
                Thrust058(Z)=Thrust(i);
                EAP058(Z)=EAP(i);
                Drag058(Z)=Drag(i);
                CTAP058(Z)=CTAP(i);
                Eavg058(Z)=Eavg(i);
                Z=Z+1;
            end
    else
    end
%     end
end

for i=1:length(phi02)
%     if mdot02(i)<=1.06 && mdot02(i)>=0.94
    if A02(i)==0.48
            if det02(i)==0
                color='r';
                phi03no02(Xno02)=phi02(i);
                mdot03no02(Xno02)=mdot02(i);
                pgain03no02(Xno02)=pgain02(i);
                det03no02(Xno02)=det02(i);
                A03no02(Xno02)=A02(i);
                Thrustno02(Xno02)=Thrust02(i);
                EAP0no02(Xno02)=EAP02(i);
                Drag0no02(Xno02)=Drag02(i);
                CTAPno02(Xno02)=CTAP02(i);
```

```matlab
                Eavgno02(Xno02)=Eavg02(i);
                Xno02=Xno02+1;
            else
                phi0302(X02)=phi02(i);
                mdot0302(X02)=mdot02(i);
                pgain0302(X02)=pgain02(i);
                det0302(X02)=det02(i);
                A0302(X02)=A02(i);
                Thrust0302(X02)=Thrust02(i);
                EAP0302(X02)=EAP02(i);
                Drag0302(X02)=Drag02(i);
                CTAP0302(X02)=CTAP02(i);
                Eavg0302(X02)=Eavg02(i);
                X02=X02+1;
            end
    elseif A02(i)==0.68
            if det02(i)==0
                color='r';
                phi045no02(Yno02)=phi02(i);
                mdot045no02(Yno02)=mdot02(i);
                pgain045no02(Yno02)=pgain02(i);
                det045no02(Yno02)=det02(i);
                A045no02(Yno02)=A02(i);
                Thrust045no02(Yno02)=Thrust02(i);
                EAP045no02(Yno02)=EAP02(i);
                Drag045no02(Yno02)=Drag02(i);
                CTAP045no02(Yno02)=CTAP02(i);
                Eavg045no02(Yno02)=Eavg02(i);
                Yno02=Yno02+1;
            else
                phi04502(Y02)=phi02(i);
                mdot04502(Y02)=mdot02(i);
                pgain04502(Y02)=pgain02(i);
                det04502(Y02)=det02(i);
                A04502(Y02)=A02(i);
                Thrust04502(Y02)=Thrust02(i);
                EAP04502(Y02)=EAP02(i);
                Drag04502(Y02)=Drag02(i);
                CTAP04502(Y02)=CTAP02(i);
                Eavg04502(Y02)=Eavg02(i);
                Y02=Y02+1;
            end
    elseif A02(i)==0.83
            if det02(i)==0
                color='r';
                phi058no02(Zno02)=phi02(i);
                mdot058no02(Zno02)=mdot02(i);
                pgain058no02(Zno02)=pgain02(i);
                det058no02(Zno02)=det02(i);
                A058no02(Zno02)=A02(i);
                Thrust058no02(Zno02)=Thrust02(i);
                EAP058no02(Zno02)=EAP02(i);
                Drag058no02(Zno02)=Drag02(i);
                CTAP058no02(Zno02)=CTAP02(i);
                Eavg058no02(Zno02)=Eavg02(i);
```

```matlab
                Zno02=Zno02+1;
            else
                phi05802(Z02)=phi02(i);
                mdot05802(Z02)=mdot02(i);
                pgain05802(Z02)=pgain02(i);
                det05802(Z02)=det02(i);
                A05802(Z02)=A02(i);
                Thrust05802(Z02)=Thrust02(i);
                EAP05802(Z02)=EAP02(i);
                Drag05802(Z02)=Drag02(i);
                CTAP05802(Z02)=CTAP02(i);
                Eavg05802(Z02)=Eavg02(i);
                Z02=Z02+1;
            end
    else
    end
%     end
end

for i=1:length(phi03)
%     if mdot03(i)<=1.06 && mdot03(i)>=0.94
    if A03(i)==0.48
            if det03(i)==0
                color='r';
                phi03no03(Xno03)=phi03(i);
                mdot03no03(Xno03)=mdot03(i);
                pgain03no03(Xno03)=pgain03(i);
                det03no03(Xno03)=det03(i);
                A03no03(Xno03)=A03(i);
                Thrustno03(Xno03)=Thrust03(i);
                EAPno03(Xno03)=EAP03(i);
                Dragno03(Xno03)=Drag03(i);
                CTAPno03(Xno03)=CTAP03(i);
                Eavgno03(Xno03)=Eavg03(i);
                Xno03=Xno03+1;
            else
                phi0303(X03)=phi03(i);
                mdot0303(X03)=mdot03(i);
                pgain0303(X03)=pgain03(i);
                det0303(X03)=det03(i);
                A0303(X03)=A03(i);
                Thrust0303(X03)=Thrust03(i);
                EAP0303(X03)=EAP03(i);
                Drag0303(X03)=Drag03(i);
                CTAP0303(X03)=CTAP03(i);
                Eavg0303(X03)=Eavg03(i);
                X03=X03+1;
            end
    elseif A03(i)==0.68
            if det03(i)==0
                color='r';
                phi045no03(Yno03)=phi03(i);
                mdot045no03(Yno03)=mdot03(i);
                pgain045no03(Yno03)=pgain03(i);
                det045no03(Yno03)=det03(i);
```

81

```matlab
                A045no03(Yno03)=A03(i);
                Thrust045no03(Yno03)=Thrust(i);
                EAP045no03(Yno03)=EAP03(i);
                Drag045no03(Yno03)=Drag03(i);
                CTAP045no03(Yno03)=CTAP03(i);
                Eavg045no03(Yno03)=Eavg03(i);
                Yno03=Yno03+1;
            else
                phi04503(Y03)=phi03(i);
                mdot04503(Y03)=mdot03(i);
                pgain04503(Y03)=pgain03(i);
                det04503(Y03)=det03(i);
                A04503(Y03)=A03(i);
                Thrust04503(Y03)=Thrust03(i);
                EAP04503(Y03)=EAP03(i);
                Drag04503(Y03)=Drag03(i);
                CTAP04503(Y03)=CTAP03(i);
                Eavg04503(Y03)=Eavg03(i);
                Y03=Y03+1;
            end
    elseif A03(i)==0.83
            if det03(i)==0
                color='r';
                phi058no03(Zno03)=phi03(i);
                mdot058no03(Zno03)=mdot03(i);
                pgain058no03(Zno03)=pgain03(i);
                det058no03(Zno03)=det03(i);
                A058no03(Zno03)=A03(i);
                Thrust058no03(Zno03)=Thrust03(i);
                EAP058no03(Zno03)=EAP03(i);
                Drag058no03(Zno03)=Drag03(i);
                CTAP058no03(Zno03)=CTAP03(i);
                Eavg058no03(Zno03)=Eavg03(i);
                Zno03=Zno03+1;
            else
                phi05803(Z03)=phi03(i);
                mdot05803(Z03)=mdot03(i);
                pgain05803(Z03)=pgain03(i);
                det05803(Z03)=det03(i);
                A05803(Z03)=A03(i);
                Thrust05803(Z03)=Thrust03(i);
                EAP05803(Z03)=EAP03(i);
                Drag05803(Z03)=Drag03(i);
                CTAP05803(Z03)=CTAP03(i);
                Eavg05803(Z03)=Eavg03(i);
                Z03=Z03+1;
            end
    else
    end
%end
end


cor03=1/((1+((1.24-1)/2)*(0.30^2))^(-1.24/.24));
cor045=1/((1+((1.24-1)/2)*(0.45^2))^(-1.24/.24));
```

```matlab
cor058=1/((1+((1.24-1)/2)*(0.58^2))^(-1.24/.24));

%% Graphing

figure;
    errx0302=linspace(22.85,22.85,length(Drag0302));
    erry0302=linspace(2.22,2.22,length(Thrust0302));

e0302=errorbar(abs(Drag0302),Thrust0302,errx0302,'horizontal','o','Mark
erEdgeColor','g','MarkerFaceColor','g');
    e0302.Color='g';
    hold on
    errx04502=linspace(22.85,22.85,length(Drag04502));
    erry04502=linspace(2.22,2.22,length(Thrust04502));

e04502=errorbar(abs(Drag04502),Thrust04502,errx04502,'horizontal','s','
MarkerEdgeColor','b','MarkerFaceColor','b');
    e04502.Color='b';
    hold on
    errx05802=linspace(22.85,22.85,length(Drag05802));
    erry05802=linspace(2.22,2.22,length(Thrust05802));

e05802=errorbar(abs(Drag05802),Thrust05802,errx05802,'horizontal','^','
MarkerEdgeColor','k','MarkerFaceColor','k');
    e05802.Color='k';
    hold on

e03022=errorbar(abs(Drag0302),Thrust0302,erry0302,'vertical','o','Marke
rEdgeColor','g','MarkerFaceColor','g');
    e03022.Color='g';
    hold on
    legend('0.48 A_8/A_3_._2','0.68 A_8/A_3_._2','0.83 A_8/A_3_._2',...
    'location','best');
    xlabel('Base Drag (N)')
    ylabel('Thrust (N)')
    title('0.30 A_3_._1/A_3_._2')
    grid on

figure;
    errx030=linspace(22.85,22.85,length(Drag030));
    erry030=linspace(2.22,2.22,length(Thrust030));

e030=errorbar(abs(Drag030),Thrust030,errx030,'horizontal','o','MarkerEd
geColor','g','MarkerFaceColor','g');
    e030.Color='g';
    hold on
    errx0302=linspace(22.85,22.85,length(Drag0302));
    erry0302=linspace(2.22,2.22,length(Thrust0302));

e0302=errorbar(abs(Drag0302),Thrust0302,errx0302,'horizontal','s','Mark
erEdgeColor','b','MarkerFaceColor','b');
    e0302.Color='b';
    hold on
    errx0303=linspace(22.85,22.85,length(Drag0303));
    erry0303=linspace(2.22,2.22,length(Thrust0303));
```

```matlab
e0303=errorbar(abs(Drag0303),Thrust0303,errx0303,'horizontal','^','Mark
erEdgeColor','k','MarkerFaceColor','k');
    e0303.Color='k';
    legend('0.30 A_3_._1/A_3_._2','0.50 A_3_._1/A_3_._2','0.58
A_3_._1/A_3_._2',...
        'location','best');
    xlabel('Base Drag (N)')
    ylabel('Thrust (N)')
    title('0.48 A_8/A_3_._2')
    grid on


CTAP030=CTAP030*cor03;
CTAP0302=CTAP0302*cor03;
CTAP0303=CTAP0303*cor03;
CTAP045=CTAP045*cor045;
CTAP058=CTAP058*cor058;
CTAP04502=CTAP04502*cor045;
CTAP05802=CTAP05802*cor058;
CTAP04503=CTAP04503*cor045;
CTAP05803=CTAP05803*cor058;


figure;
%     errx030=linspace(6.0,6.0,length(Drag030));
%     erry030=linspace(5.7,5.7,length(Thrust030));
%
e030=errorbar(EAP030,CTAP030,errx030,'horizontal','o','MarkerEdgeColor'
,'g','MarkerFaceColor','g');
%     e030.Color='g';
    scatter(EAP030,CTAP030,'o','g','filled')
    hold on
%     errx045=linspace(4.3,4.3,length(Drag045));
%     erry045=linspace(5.7,5.7,length(Thrust045));
%
e045=errorbar(EAP045,CTAP045,errx045,'horizontal','o','MarkerEdgeColor'
,'b','MarkerFaceColor','b');
%     e045.Color='b';
    scatter(EAP045,CTAP045,'o','b','filled')
    hold on
%     errx058=linspace(3.5,3.5,length(Drag058));
%     erry058=linspace(5.7,5.7,length(Thrust058));
%
e058=errorbar(EAP058,CTAP058,errx058,'horizontal','o','MarkerEdgeColor'
,'k','MarkerFaceColor','k');
%     e058.Color='k';
    scatter(EAP058,CTAP058,'o','k','filled')
    hold on
    xxxx=1:1200;
    plot(xxxx,xxxx)
    hold on
    scatter(EAP0302,CTAP0302,'o','g','filled')
    hold on
    scatter(EAP04502,CTAP04502,'o','b','filled')
```

```matlab
    hold on
    scatter(EAP05802,CTAP05802,'o','k','filled')
    hold on
    scatter(EAP0303,CTAP0303,'o','g','filled')
    hold on
    scatter(EAP04503,CTAP04503,'o','b','filled')
    hold on
    scatter(EAP05803,CTAP05803,'o','k','filled')
    legend('0.48 A_8/A_3_._2','0.68 A_8/A_3_._2','0.83 A_8/A_3_._2',...
        'location','best','fontsize',12,'fontweight','bold');
    xlabel('P_T_8 Theoretical (kPa)','fontsize',12,'fontweight','bold')
    ylabel('P_T_6 Experimental
(kPa)','fontsize',12,'fontweight','bold')
    grid on




clear all
close all
clc

%% Excel Read In

phi=xlsread('ThesisData.xlsx','D4:D49');
mdot=xlsread('ThesisData.xlsx','C4:C49');
A=xlsread('ThesisData.xlsx','E4:E49');
pgain=xlsread('ThesisData.xlsx','K4:K49');
det=xlsread('ThesisData.xlsx','L4:L49');
Thrust=xlsread('ThesisData.xlsx','F4:F49');
EAP=xlsread('ThesisData.xlsx','J4:J49');
Drag=xlsread('ThesisData.xlsx','H4:H49');
CTAP=xlsread('ThesisData.xlsx','G4:G49');
Eavg=xlsread('ThesisData.xlsx','Y4:Y49');
Thrust=Thrust-Drag;



phi02=xlsread('ThesisData.xlsx','D51:D61');
mdot02=xlsread('ThesisData.xlsx','C51:C61');
A02=xlsread('ThesisData.xlsx','E51:E61');
pgain02=xlsread('ThesisData.xlsx','K51:K61');
det02=xlsread('ThesisData.xlsx','L51:L61');
Thrust02=xlsread('ThesisData.xlsx','F51:F61');
EAP02=xlsread('ThesisData.xlsx','J51:J61');
Drag02=xlsread('ThesisData.xlsx','H51:H61');
CTAP02=xlsread('ThesisData.xlsx','G51:G61');
Eavg02=xlsread('ThesisData.xlsx','Y51:Y61');
Thrust02=Thrust02-Drag02;



phi03=xlsread('ThesisData.xlsx','D63:D73');
mdot03=xlsread('ThesisData.xlsx','C63:C73');
A03=xlsread('ThesisData.xlsx','E63:E73');
pgain03=xlsread('ThesisData.xlsx','K63:K73');
det03=xlsread('ThesisData.xlsx','L63:L73');
```

```matlab
Thrust03=xlsread('ThesisData.xlsx','F63:F73');
EAP03=xlsread('ThesisData.xlsx','J63:J73');
Drag03=xlsread('ThesisData.xlsx','H63:H73');
CTAP03=xlsread('ThesisData.xlsx','G63:G73');
Eavg03=xlsread('ThesisData.xlsx','Y63:Y73');
Thrust03=Thrust03-Drag03;
%% Numbering Initial Values
X=1;
Y=1;
Z=1;
Xno=1;
Yno=1;
Zno=1;
X02=1;
Y02=1;
Z02=1;
Xno02=1;
Yno02=1;
Zno02=1;
X03=1;
Y03=1;
Z03=1;
Xno03=1;
Yno03=1;
Zno03=1;


%% Seperation of Data


for i=1:length(phi)
    if mdot(i)<=1.06 && mdot(i)>=0.94

    if A(i)==0.48
            if det(i)==0
                color='r';
                phi03no(Xno)=phi(i);
                mdot03no(Xno)=mdot(i);
                pgain03no(Xno)=pgain(i);
                det03no(Xno)=det(i);
                A03no(Xno)=A(i);
                Thrustno(Xno)=Thrust(i);
                EAPno(Xno)=EAP(i);
                Dragno(Xno)=Drag(i);
                CTAPno(Xno)=CTAP(i);
                Eavgno(Xno)=Eavg(i);
                Xno=Xno+1;
            else
                phi030(X)=phi(i);
                mdot030(X)=mdot(i);
                pgain030(X)=pgain(i);
                det030(X)=det(i);
                A030(X)=A(i);
                Thrust030(X)=Thrust(i);
                EAP030(X)=EAP(i);
                Drag030(X)=Drag(i);
                CTAP030(X)=CTAP(i);
```

```
                Eavg030(X)=Eavg(i);
                X=X+1;
            end
    elseif A(i)==0.68
        color='b';
            if det(i)==0
                color='r';
                phi045no(Yno)=phi(i);
                mdot045no(Yno)=mdot(i);
                pgain045no(Yno)=pgain(i);
                det045no(Yno)=det(i);
                A045no(Yno)=A(i);
                Thrust045no(Yno)=Thrust(i);
                EAP045no(Yno)=EAP(i);
                Drag045no(Yno)=Drag(i);
                CTAP045no(Yno)=CTAP(i);
                Eavg045no(Yno)=Eavg(i);
                Yno=Yno+1;
            else
                phi045(Y)=phi(i);
                mdot045(Y)=mdot(i);
                pgain045(Y)=pgain(i);
                det045(Y)=det(i);
                A045(Y)=A(i);
                Thrust045(Y)=Thrust(i);
                EAP045(Y)=EAP(i);
                Drag045(Y)=Drag(i);
                CTAP045(Y)=CTAP(i);
                Eavg045(Y)=Eavg(i);
                Y=Y+1;
            end
    elseif A(i)==0.83
            if det(i)==0
                color='r';
                phi058no(Zno)=phi(i);
                mdot058no(Zno)=mdot(i);
                pgain058no(Zno)=pgain(i);
                det058no(Zno)=det(i);
                A058no(Zno)=A(i);
                Thrust058no(Zno)=Thrust(i);
                EAP058no(Zno)=EAP(i);
                Drag058no(Zno)=Drag(i);
                CTAP058no(Zno)=CTAP(i);
                Eavg058no(Zno)=Eavg(i);
                Zno=Zno+1;
            else
                phi058(Z)=phi(i);
                mdot058(Z)=mdot(i);
                pgain058(Z)=pgain(i);
                det058(Z)=det(i);
                A058(Z)=A(i);
                Thrust058(Z)=Thrust(i);
                EAP058(Z)=EAP(i);
                Drag058(Z)=Drag(i);
                CTAP058(Z)=CTAP(i);
```

```matlab
                    Eavg058(Z)=Eavg(i);
                    Z=Z+1;
                end
        else
        end
        end
end

for i=1:length(phi02)
    if mdot02(i)<=1.06 && mdot02(i)>=0.94
    if A02(i)==0.48
            if det02(i)==0
                color='r';
                phi03no02(Xno02)=phi02(i);
                mdot03no02(Xno02)=mdot02(i);
                pgain03no02(Xno02)=pgain02(i);
                det03no02(Xno02)=det02(i);
                A03no02(Xno02)=A02(i);
                Thrustno02(Xno02)=Thrust02(i);
                EAP0no02(Xno02)=EAP02(i);
                Drag0no02(Xno02)=Drag02(i);
                CTAPno02(Xno02)=CTAP02(i);
                Eavgno02(Xno02)=Eavg02(i);
                Xno02=Xno02+1;
            else
                phi0302(X02)=phi02(i);
                mdot0302(X02)=mdot02(i);
                pgain0302(X02)=pgain02(i);
                det0302(X02)=det02(i);
                A0302(X02)=A02(i);
                Thrust0302(X02)=Thrust02(i);
                EAP0302(X02)=EAP02(i);
                Drag0302(X02)=Drag02(i);
                CTAP0302(X02)=CTAP02(i);
                Eavg0302(X02)=Eavg02(i);
                X02=X02+1;
            end
    elseif A02(i)==0.68
            if det02(i)==0
                color='r';
                phi045no02(Yno02)=phi02(i);
                mdot045no02(Yno02)=mdot02(i);
                pgain045no02(Yno02)=pgain02(i);
                det045no02(Yno02)=det02(i);
                A045no02(Yno02)=A02(i);
                Thrust045no02(Yno02)=Thrust02(i);
                EAP045no02(Yno02)=EAP02(i);
                Drag045no02(Yno02)=Drag02(i);
                CTAP045no02(Yno02)=CTAP02(i);
                Eavg045no02(Yno02)=Eavg02(i);
                Yno02=Yno02+1;
            else
                phi04502(Y02)=phi02(i);
                mdot04502(Y02)=mdot02(i);
                pgain04502(Y02)=pgain02(i);
```

```matlab
                    det04502(Y02)=det02(i);
                    A04502(Y02)=A02(i);
                    Thrust04502(Y02)=Thrust02(i);
                    EAP04502(Y02)=EAP02(i);
                    Drag04502(Y02)=Drag02(i);
                    CTAP04502(Y02)=CTAP02(i);
                    Eavg04502(Y02)=Eavg02(i);
                    Y02=Y02+1;
                end
        elseif A02(i)==0.83
                if det02(i)==0
                    color='r';
                    phi058no02(Zno02)=phi02(i);
                    mdot058no02(Zno02)=mdot02(i);
                    pgain058no02(Zno02)=pgain02(i);
                    det058no02(Zno02)=det02(i);
                    A058no02(Zno02)=A02(i);
                    Thrust058no02(Zno02)=Thrust02(i);
                    EAP058no02(Zno02)=EAP02(i);
                    Drag058no02(Zno02)=Drag02(i);
                    CTAP058no02(Zno02)=CTAP02(i);
                    Eavg058no02(Zno02)=Eavg02(i);
                    Zno02=Zno02+1;
                else
                    phi05802(Z02)=phi02(i);
                    mdot05802(Z02)=mdot02(i);
                    pgain05802(Z02)=pgain02(i);
                    det05802(Z02)=det02(i);
                    A05802(Z02)=A02(i);
                    Thrust05802(Z02)=Thrust02(i);
                    EAP05802(Z02)=EAP02(i);
                    Drag05802(Z02)=Drag02(i);
                    CTAP05802(Z02)=CTAP02(i);
                    Eavg05802(Z02)=Eavg02(i);
                    Z02=Z02+1;
                end
        else
        end
        end
end

for i=1:length(phi03)
    if mdot03(i)<=1.06 && mdot03(i)>=0.94
    if A03(i)==0.48
            if det03(i)==0
                color='r';
                phi03no03(Xno03)=phi03(i);
                mdot03no03(Xno03)=mdot03(i);
                pgain03no03(Xno03)=pgain03(i);
                det03no03(Xno03)=det03(i);
                A03no03(Xno03)=A03(i);
                Thrustno03(Xno03)=Thrust03(i);
                EAPno03(Xno03)=EAP03(i);
                Dragno03(Xno03)=Drag03(i);
                CTAPno03(Xno03)=CTAP03(i);
```

89

```matlab
            Eavgno03(Xno03)=Eavg03(i);
            Xno03=Xno03+1;
        else
            phi0303(X03)=phi03(i);
            mdot0303(X03)=mdot03(i);
            pgain0303(X03)=pgain03(i);
            det0303(X03)=det03(i);
            A0303(X03)=A03(i);
            Thrust0303(X03)=Thrust03(i);
            EAP0303(X03)=EAP03(i);
            Drag0303(X03)=Drag03(i);
            CTAP0303(X03)=CTAP03(i);
            Eavg0303(X03)=Eavg03(i);
            X03=X03+1;
        end
elseif A03(i)==0.68
        if det03(i)==0
            color='r';
            phi045no03(Yno03)=phi03(i);
            mdot045no03(Yno03)=mdot03(i);
            pgain045no03(Yno03)=pgain03(i);
            det045no03(Yno03)=det03(i);
            A045no03(Yno03)=A03(i);
            Thrust045no03(Yno03)=Thrust(i);
            EAP045no03(Yno03)=EAP03(i);
            Drag045no03(Yno03)=Drag03(i);
            CTAP045no03(Yno03)=CTAP03(i);
            Eavg045no03(Yno03)=Eavg03(i);
            Yno03=Yno03+1;
        else
            phi04503(Y03)=phi03(i);
            mdot04503(Y03)=mdot03(i);
            pgain04503(Y03)=pgain03(i);
            det04503(Y03)=det03(i);
            A04503(Y03)=A03(i);
            Thrust04503(Y03)=Thrust03(i);
            EAP04503(Y03)=EAP03(i);
            Drag04503(Y03)=Drag03(i);
            CTAP04503(Y03)=CTAP03(i);
            Eavg04503(Y03)=Eavg03(i);
            Y03=Y03+1;
        end
elseif A03(i)==0.83
        if det03(i)==0
            color='r';
            phi058no03(Zno03)=phi03(i);
            mdot058no03(Zno03)=mdot03(i);
            pgain058no03(Zno03)=pgain03(i);
            det058no03(Zno03)=det03(i);
            A058no03(Zno03)=A03(i);
            Thrust058no03(Zno03)=Thrust03(i);
            EAP058no03(Zno03)=EAP03(i);
            Drag058no03(Zno03)=Drag03(i);
            CTAP058no03(Zno03)=CTAP03(i);
            Eavg058no03(Zno03)=Eavg03(i);
```

```matlab
                    Zno03=Zno03+1;
                else
                    phi05803(Z03)=phi03(i);
                    mdot05803(Z03)=mdot03(i);
                    pgain05803(Z03)=pgain03(i);
                    det05803(Z03)=det03(i);
                    A05803(Z03)=A03(i);
                    Thrust05803(Z03)=Thrust03(i);
                    EAP05803(Z03)=EAP03(i);
                    Drag05803(Z03)=Drag03(i);
                    CTAP05803(Z03)=CTAP03(i);
                    Eavg05803(Z03)=Eavg03(i);
                    Z03=Z03+1;
                end
        else
        end
end
end

figure;

e030=errorbar(phi030,pgain030,Eavg030,'vertical','o','MarkerEdgeColor',
'g','MarkerFaceColor','g');
    e030.Color='g';
%     scatter(phi030,pgain030,'o','g','filled')
    xlabel('Equivalence Ratio')
    ylabel('Pressure Gain (%)')
    grid on
    hold on

e045=errorbar(phi045,pgain045,Eavg045,'vertical','s','MarkerEdgeColor',
'b','MarkerFaceColor','b');
    e045.Color='b';
%     scatter(phi045,pgain045,'s','b','filled')
    hold on

e058=errorbar(phi058,pgain058,Eavg058,'vertical','^','MarkerEdgeColor',
'k','MarkerFaceColor','k');
    e058.Color='k';
%     scatter(phi058,pgain058,'^','k','filled')
    hold on
%
e03no=errorbar(phi03no,pgain03no,Eavg03no,'vertical','o','MarkerEdgeCol
or','r','MarkerFaceColor','r');
%     e03no.Color='r';
    scatter(phi03no,pgain03no,'o','r','filled')
    legend('0.48 A_8/A_3_._2','0.68 A_8/A_3_._2','0.83 A_8/A_3_._2',...
        'No Detonation','location','best');
    title('Constant Mass Flowrate 1.0kg/s for 0.30 A_3_._1/A_3_._2')
    xlim([0.6 1.2])
    ylim([-40 0])

figure;
```

```matlab
e045=errorbar(phi045,pgain045,Eavg045,'vertical','o','MarkerEdgeColor',
'g','MarkerFaceColor','g');
    e045.Color='g';
%   scatter(phi045,pgain045,'o','g','filled')
    hold on

e04502=errorbar(phi04502,pgain04502,Eavg04502,'vertical','s','MarkerEdg
eColor','b','MarkerFaceColor','b');
    e04502.Color='b';
%       scatter(phi04502,pgain04502,'s','b','filled')

    hold on

e04503=errorbar(phi04503,pgain04503,Eavg04503,'vertical','^','MarkerEdg
eColor','k','MarkerFaceColor','k');
    e04503.Color='k';
    hold on
    scatter(phi045no02,pgain045no02,'s','r','filled')
%       scatter(phi04503,pgain04503,'^','k','filled')
    xlabel('Equivalence Ratio')
    ylabel('Pressure Gain (%)')
    grid on
    legend('0.3 A_3_._1/A_3_._2','0.5 A_3_._1/A_3_._2',...
        '0.57 A_3_._1/A_3_._2','No Detonation','location','best');
    title('Constant Mass Flowrate 1.0kg/s for 0.68 A_8/A_3_._2')
    xlim([0.6 1.2])
    ylim([-40 0])

clear all
close all
clc

%% Excel Read In

phi=xlsread('ThesisData.xlsx','D4:D49');
mdot=xlsread('ThesisData.xlsx','C4:C49');
A=xlsread('ThesisData.xlsx','E4:E49');
pgain=xlsread('ThesisData.xlsx','K4:K49');
det=xlsread('ThesisData.xlsx','L4:L49');
Thrust=xlsread('ThesisData.xlsx','F4:F49');
EAP=xlsread('ThesisData.xlsx','J4:J49');
Drag=xlsread('ThesisData.xlsx','H4:H49');
CTAP=xlsread('ThesisData.xlsx','G4:G49');
Eavg=xlsread('ThesisData.xlsx','Y4:Y49');
Thrust=Thrust-Drag;


phi02=xlsread('ThesisData.xlsx','D51:D61');
mdot02=xlsread('ThesisData.xlsx','C51:C61');
A02=xlsread('ThesisData.xlsx','E51:E61');
pgain02=xlsread('ThesisData.xlsx','K51:K61');
det02=xlsread('ThesisData.xlsx','L51:L61');
Thrust02=xlsread('ThesisData.xlsx','F51:F61');
```

```matlab
EAP02=xlsread('ThesisData.xlsx','J51:J61');
Drag02=xlsread('ThesisData.xlsx','H51:H61');
CTAP02=xlsread('ThesisData.xlsx','G51:G61');
Eavg02=xlsread('ThesisData.xlsx','Y51:Y61');
Thrust02=Thrust02-Drag02;


phi03=xlsread('ThesisData.xlsx','D63:D73');
mdot03=xlsread('ThesisData.xlsx','C63:C73');
A03=xlsread('ThesisData.xlsx','E63:E73');
pgain03=xlsread('ThesisData.xlsx','K63:K73');
det03=xlsread('ThesisData.xlsx','L63:L73');
Thrust03=xlsread('ThesisData.xlsx','F63:F73');
EAP03=xlsread('ThesisData.xlsx','J63:J73');
Drag03=xlsread('ThesisData.xlsx','H63:H73');
CTAP03=xlsread('ThesisData.xlsx','G63:G73');
Eavg03=xlsread('ThesisData.xlsx','Y63:Y73');
Thrust03=Thrust03-Drag03;
%% Numbering Initial Values
X=1;
Y=1;
Z=1;
Xno=1;
Yno=1;
Zno=1;
X02=1;
Y02=1;
Z02=1;
Xno02=1;
Yno02=1;
Zno02=1;
X03=1;
Y03=1;
Z03=1;
Xno03=1;
Yno03=1;
Zno03=1;

%% Seperation of Data

for i=1:length(phi)
    if phi(i)<=1.06 && phi(i)>=0.94

    if A(i)==0.48
            if det(i)==0
                color='r';
                phi03no(Xno)=phi(i);
                mdot03no(Xno)=mdot(i);
                pgain03no(Xno)=pgain(i);
                det03no(Xno)=det(i);
                A03no(Xno)=A(i);
                Thrustno(Xno)=Thrust(i);
                EAPno(Xno)=EAP(i);
                Dragno(Xno)=Drag(i);
```

```matlab
            CTAPno(Xno)=CTAP(i);
            Eavgno(Xno)=Eavg(i);
            Xno=Xno+1;
        else
            phi030(X)=phi(i);
            mdot030(X)=mdot(i);
            pgain030(X)=pgain(i);
            det030(X)=det(i);
            A030(X)=A(i);
            Thrust030(X)=Thrust(i);
            EAP030(X)=EAP(i);
            Drag030(X)=Drag(i);
            CTAP030(X)=CTAP(i);
            Eavg030(X)=Eavg(i);
            X=X+1;
        end
elseif A(i)==0.68
    color='b';
        if det(i)==0
            color='r';
            phi045no(Yno)=phi(i);
            mdot045no(Yno)=mdot(i);
            pgain045no(Yno)=pgain(i);
            det045no(Yno)=det(i);
            A045no(Yno)=A(i);
            Thrust045no(Yno)=Thrust(i);
            EAP045no(Yno)=EAP(i);
            Drag045no(Yno)=Drag(i);
            CTAP045no(Yno)=CTAP(i);
            Eavg045no(Yno)=Eavg(i);
            Yno=Yno+1;
        else
            phi045(Y)=phi(i);
            mdot045(Y)=mdot(i);
            pgain045(Y)=pgain(i);
            det045(Y)=det(i);
            A045(Y)=A(i);
            Thrust045(Y)=Thrust(i);
            EAP045(Y)=EAP(i);
            Drag045(Y)=Drag(i);
            CTAP045(Y)=CTAP(i);
            Eavg045(Y)=Eavg(i);
            Y=Y+1;
        end
elseif A(i)==0.83
        if det(i)==0
            color='r';
            phi058no(Zno)=phi(i);
            mdot058no(Zno)=mdot(i);
            pgain058no(Zno)=pgain(i);
            det058no(Zno)=det(i);
            A058no(Zno)=A(i);
            Thrust058no(Zno)=Thrust(i);
            EAP058no(Zno)=EAP(i);
            Drag058no(Zno)=Drag(i);
```

```matlab
                    CTAP058no(Zno)=CTAP(i);
                    Eavg058no(Zno)=Eavg(i);
                    Zno=Zno+1;
                else
                    phi058(Z)=phi(i);
                    mdot058(Z)=mdot(i);
                    pgain058(Z)=pgain(i);
                    det058(Z)=det(i);
                    A058(Z)=A(i);
                    Thrust058(Z)=Thrust(i);
                    EAP058(Z)=EAP(i);
                    Drag058(Z)=Drag(i);
                    CTAP058(Z)=CTAP(i);
                    Eavg058(Z)=Eavg(i);
                    Z=Z+1;
                end
        else
        end
        end
end

for i=1:length(phi02)
    if phi02(i)<=1.06 && phi02(i)>=0.94
    if A02(i)==0.48
            if det02(i)==0
                color='r';
                phi03no02(Xno02)=phi02(i);
                mdot03no02(Xno02)=mdot02(i);
                pgain03no02(Xno02)=pgain02(i);
                det03no02(Xno02)=det02(i);
                A03no02(Xno02)=A02(i);
                Thrustno02(Xno02)=Thrust02(i);
                EAP0no02(Xno02)=EAP02(i);
                Drag0no02(Xno02)=Drag02(i);
                CTAPno02(Xno02)=CTAP02(i);
                Eavgno02(Xno02)=Eavg02(i);
                Xno02=Xno02+1;
            else
                phi0302(X02)=phi02(i);
                mdot0302(X02)=mdot02(i);
                pgain0302(X02)=pgain02(i);
                det0302(X02)=det02(i);
                A0302(X02)=A02(i);
                Thrust0302(X02)=Thrust02(i);
                EAP0302(X02)=EAP02(i);
                Drag0302(X02)=Drag02(i);
                CTAP0302(X02)=CTAP02(i);
                Eavg0302(X02)=Eavg02(i);
                X02=X02+1;
            end
    elseif A02(i)==0.68
            if det02(i)==0
                color='r';
                phi045no02(Yno02)=phi02(i);
                mdot045no02(Yno02)=mdot02(i);
```

95

```matlab
                pgain045no02(Yno02)=pgain02(i);
                det045no02(Yno02)=det02(i);
                A045no02(Yno02)=A02(i);
                Thrust045no02(Yno02)=Thrust02(i);
                EAP045no02(Yno02)=EAP02(i);
                Drag045no02(Yno02)=Drag02(i);
                CTAP045no02(Yno02)=CTAP02(i);
                Eavg045no02(Yno02)=Eavg02(i);
                Yno02=Yno02+1;
            else
                phi04502(Y02)=phi02(i);
                mdot04502(Y02)=mdot02(i);
                pgain04502(Y02)=pgain02(i);
                det04502(Y02)=det02(i);
                A04502(Y02)=A02(i);
                Thrust04502(Y02)=Thrust02(i);
                EAP04502(Y02)=EAP02(i);
                Drag04502(Y02)=Drag02(i);
                CTAP04502(Y02)=CTAP02(i);
                Eavg04502(Y02)=Eavg02(i);
                Y02=Y02+1;
            end
    elseif A02(i)==0.83
            if det02(i)==0
                color='r';
                phi058no02(Zno02)=phi02(i);
                mdot058no02(Zno02)=mdot02(i);
                pgain058no02(Zno02)=pgain02(i);
                det058no02(Zno02)=det02(i);
                A058no02(Zno02)=A02(i);
                Thrust058no02(Zno02)=Thrust02(i);
                EAP058no02(Zno02)=EAP02(i);
                Drag058no02(Zno02)=Drag02(i);
                CTAP058no02(Zno02)=CTAP02(i);
                Eavg058no02(Zno02)=Eavg02(i);
                Zno02=Zno02+1;
            else
                phi05802(Z02)=phi02(i);
                mdot05802(Z02)=mdot02(i);
                pgain05802(Z02)=pgain02(i);
                det05802(Z02)=det02(i);
                A05802(Z02)=A02(i);
                Thrust05802(Z02)=Thrust02(i);
                EAP05802(Z02)=EAP02(i);
                Drag05802(Z02)=Drag02(i);
                CTAP05802(Z02)=CTAP02(i);
                Eavg05802(Z02)=Eavg02(i);
                Z02=Z02+1;
            end
    else
    end
    end
end

for i=1:length(phi03)
```

```matlab
if phi03(i)<=1.06 && phi03(i)>=0.94
if A03(i)==0.48
        if det03(i)==0
            color='r';
            phi03no03(Xno03)=phi03(i);
            mdot03no03(Xno03)=mdot03(i);
            pgain03no03(Xno03)=pgain03(i);
            det03no03(Xno03)=det03(i);
            A03no03(Xno03)=A03(i);
            Thrustno03(Xno03)=Thrust03(i);
            EAPno03(Xno03)=EAP03(i);
            Dragno03(Xno03)=Drag03(i);
            CTAPno03(Xno03)=CTAP03(i);
            Eavgno03(Xno03)=Eavg03(i);
            Xno03=Xno03+1;
        else
            phi0303(X03)=phi03(i);
            mdot0303(X03)=mdot03(i);
            pgain0303(X03)=pgain03(i);
            det0303(X03)=det03(i);
            A0303(X03)=A03(i);
            Thrust0303(X03)=Thrust03(i);
            EAP0303(X03)=EAP03(i);
            Drag0303(X03)=Drag03(i);
            CTAP0303(X03)=CTAP03(i);
            Eavg0303(X03)=Eavg03(i);
            X03=X03+1;
        end
elseif A03(i)==0.68
        if det03(i)==0
            color='r';
            phi045no03(Yno03)=phi03(i);
            mdot045no03(Yno03)=mdot03(i);
            pgain045no03(Yno03)=pgain03(i);
            det045no03(Yno03)=det03(i);
            A045no03(Yno03)=A03(i);
            Thrust045no03(Yno03)=Thrust(i);
            EAP045no03(Yno03)=EAP03(i);
            Drag045no03(Yno03)=Drag03(i);
            CTAP045no03(Yno03)=CTAP03(i);
            Eavg045no03(Yno03)=Eavg03(i);
            Yno03=Yno03+1;
        else
            phi04503(Y03)=phi03(i);
            mdot04503(Y03)=mdot03(i);
            pgain04503(Y03)=pgain03(i);
            det04503(Y03)=det03(i);
            A04503(Y03)=A03(i);
            Thrust04503(Y03)=Thrust03(i);
            EAP04503(Y03)=EAP03(i);
            Drag04503(Y03)=Drag03(i);
            CTAP04503(Y03)=CTAP03(i);
            Eavg04503(Y03)=Eavg03(i);
            Y03=Y03+1;
        end
```

```matlab
        elseif A03(i)==0.83
                if det03(i)==0
                    color='r';
                    phi058no03(Zno03)=phi03(i);
                    mdot058no03(Zno03)=mdot03(i);
                    pgain058no03(Zno03)=pgain03(i);
                    det058no03(Zno03)=det03(i);
                    A058no03(Zno03)=A03(i);
                    Thrust058no03(Zno03)=Thrust03(i);
                    EAP058no03(Zno03)=EAP03(i);
                    Drag058no03(Zno03)=Drag03(i);
                    CTAP058no03(Zno03)=CTAP03(i);
                    Eavg058no03(Zno03)=Eavg03(i);
                    Zno03=Zno03+1;
                else
                    phi05803(Z03)=phi03(i);
                    mdot05803(Z03)=mdot03(i);
                    pgain05803(Z03)=pgain03(i);
                    det05803(Z03)=det03(i);
                    A05803(Z03)=A03(i);
                    Thrust05803(Z03)=Thrust03(i);
                    EAP05803(Z03)=EAP03(i);
                    Drag05803(Z03)=Drag03(i);
                    CTAP05803(Z03)=CTAP03(i);
                    Eavg05803(Z03)=Eavg03(i);
                    Z03=Z03+1;
                end
        else
        end
end
end

figure;

e0303=errorbar(mdot0303,pgain0303,Eavg0303,'vertical','o','MarkerEdgeCo
lor','g','MarkerFaceColor','g');
    e0303.Color='g';
%     scatter(mdot0303,pgain0303,'o','g','filled')
    hold on

e04503=errorbar(mdot04503,pgain04503,Eavg04503,'vertical','s','MarkerEd
geColor','b','MarkerFaceColor','b');
    e04503.Color='b';
%     scatter(mdot04503,pgain04503,'s','b','filled')
    hold on

e05803=errorbar(mdot05803,pgain05803,Eavg05803,'vertical','^','MarkerEd
geColor','k','MarkerFaceColor','k');
    e05803.Color='k';
%     scatter(mdot05803,pgain05803,'^','k','filled')
    grid on
    legend('0.48 A_8/A_3_._2','0.68 A_8/A_3_._2','0.83
A_8/A_3_._2','location','best');
    title('Constant Phi 1.0 for 0.57 A_3_._1/A_3_._2')
    xlabel('Mass Flowrate (kg/s)')
```

```matlab
    ylabel('Pressure Gain (%)')
    grid on
    xlim([0.5 1.5])
    ylim([-40 0])
    xticks([0.5 0.75 1.0 1.25 1.5])

figure;

e045=errorbar(mdot045,pgain045,Eavg045,'vertical','o','MarkerEdgeColor'
,'g','MarkerFaceColor','g');
    e045.Color='g';
%    scatter(mdot045,pgain045,'o','g','filled')
    hold on

e04502=errorbar(mdot04502,pgain04502,Eavg04502,'vertical','s','MarkerEd
geColor','b','MarkerFaceColor','b');
    e04502.Color='b';
%     scatter(mdot04502,pgain04502,'s','b','filled')
    hold on

e04503=errorbar(mdot04503,pgain04503,Eavg04503,'vertical','^','MarkerEd
geColor','k','MarkerFaceColor','k');
    e04503.Color='k';
%     scatter(mdot04503,pgain04503,'^','k','filled')
    grid on
    legend('0.3 A_3_._1/A_3_._2','0.5 A_3_._1/A_3_._2',...
        '0.57 A_3_._1/A_3_._2','location','best');
    title('Constant Phi 1.0 for 0.68 A_8/A_3_._2')
    xlabel('Mass Flowrate (kg/s)')
    ylabel('Pressure Gain (%)')
    xlim([0.5 1.5])
    ylim([-40 0])
    xticks([0.5 0.75 1.0 1.25 1.5])
```

THIS PAGE INTENTIONALLY LEFT BLANK

LIST OF REFERENCES

[1]   D. A. Schwer and K. Kailasanath, "Rotating detonation-wave engines," 2011 *Naval Research Laboratory Review*, Washington, DC, 2011, pp. 88–94.

[2]   L. Langston, *Detonation Gas Turbines*, ASME. Mechanical Engineering. 2013.

[3]   J. H. S. Lee, *The Detonation Phenomenon*. New York, NY: Cambridge University Press, 2008.

[4]   W. H. Heiser and D. T. Pratt, "Thermodynamic cycle analysis of Pulse Detonation Engines," *Journal of Propulsion and Power*, vol. 18, no. 1, 2002.

[5]   D. A. Schwer and K. Kailasanath, "Fuel effects on Rotating Detonation Engines," 2011 Naval Research Laboratory, Washington, DC, 2011, pp. 5.

[6]   T. A. Kaemming and D. E. Paxson, "Determining the pressure gain of Pressure Gain Combustion," *2018 Joint Propulsion Conference*, AIAA Propulsion and Energy Forum, (AIAA 2018–4567)

[7]   T. L. Papatheodore and O. E. B. Messer, "On numerical considerations for modeling reactive astrophysical shocks," *The Astrophysical Journal*, vol. 782, no. 1, p. 12, 2014.

[8]   G. P. Sutton, O. Biblarz, *Rocket Propulsion Elements*. Hoboken, NJ: Wiley, 2017

[9]   J. A. Nicholls and R. B. Morrison, "Intermediate detonation as a thrust producing mechanism," *Jet Propulsion*, vol. 27, no. 5, 1957.

[10]   Patent application for RDE by Mitsubishi Heavy Industries, June 29, 2004.

[11]   R. H. Kelso, "Investigation of aerospike nozzle performance in Rotating Detonation Engines," thesis, 2018.

[12]   B. A. Rankin, J. P. Gore, J. L. Hoke, and F. R. Schauer, "Temperature estimates of exhaust plumes from a turbine driven by Pulsed Detonations," *Journal of Propulsion and Power*, vol. 30, no. 5, pp. 1438–1443, 2014.

[13]   K. Y. Cho, J. R. Codoni, B. A. Rankin, J. Hoke, and F. Schauer, "High-repetition-rate chemiluminescence imaging of a Rotating Detonation Engine," *54th AIAA Aerospace Sciences Meeting*, 2016.

[14]   A. Naples, J. Hoke, J. Karnesky, and F. Schauer, "Flowfield characterization of a Rotating Detonation Engine," *51st AIAA Aerospace Sciences Meeting including the New Horizons Forum and Aerospace Exposition*, 2013.

[15]   D. E. Paxson, M. Fotia, J. Hoke, and F. Schauer, "Comparison of numerically simulated and experimentally measured performance of a Rotating Detonation Engine," *53rd AIAA Aerospace Sciences Meeting*, 2015.

[16]   W. H. Heiser and D. T. Pratt, *Hypersonic Airbreathing Propulsion*, Washington, DC: AIAA, 1994.

[17]   R. D. Zucker, *Fundamentals of Gas Dynamics*. New York: John Wiley & Sons, Inc., 2003.

[18]   Paxson, D.E., Kaemming, T.A., "Foundational performance analyses of Pressure Gain Combustion thermodynamic benefits for gas turbines," *NASA Technical Reports Server*. AIAA 2012–0770, January 2012.

[19]   C. A. Stevens, M. Fotia, J. H., and F. Schauer. "Comparison of transient response of pressure measurement techniques with application to detonation waves," *53rd AIAA Aerospace Sciences Meeting*, AIAA SciTech Forum, (AIAA 2015–1102)

[20]   C. M. Brophy, J.R. Codoni, "Experimental Performance Characterization of an RDE Using Equivalent Available Pressure," *55th AIAA/SAE/ASEE Joint Propulsion Conference*, Indianapolis, IN, 19–23 Aug., 2019.

[21]   Omega Engineering, "Thin film pressure transducer gage, vacuum and compound ranges," Omega, 2019. [Online].

[22]   R. A. Duerr and V. J. Lyons, "Effect of flameholder pressure drop on emissions and performance of premixed prevaporized combustors," *NASA Technical Paper*. Apr. 1983.

INITIAL DISTRIBUTION LIST

1.   Defense Technical Information Center
        Ft. Belvoir, Virginia

2.   Dudley Knox Library
        Naval Postgraduate School
        Monterey, California